TÜBİTAK

Turkish Journal of Earth Sciences

http://journals.tubitak.gov.tr/earth/

Research Article

Turkish J Earth Sci
(2014) 23: 361-385
© TÜBİTAK
doi:10.3906/yer-1309-12

Tectonosedimentary evolution of the Karacasu and Bozdoğan basins in the Central Menderes Massif, W Anatolia

Faruk OCAKOĞLU[1,*], Sanem AÇIKALIN[2], Erman ÖZSAYIN[3], Ramazan Kadir DİRİK[3]

[1]Department of Geological Engineering, Eskişehir Osmangazi University, Eskişehir, Turkey
[2]Badley Ashton and Associates Ltd., Winceby House Head Office, Winceby, UK
[3]Department of Geological Engineering, Hacettepe University, Ankara, Turkey

Received: 19.09.2013 • **Accepted:** 23.05.2014 • **Published Online:** 17.06.2014 • **Printed:** 16.07.2014

Abstract: The Karacasu and Bozdoğan basins, which trend obliquely to modern grabens in the Central Menderes Massif, are investigated in terms of morphology, basinfill architecture, and structure. Evaluation of the previous geophysical and new structural data indicates that the basins are symmetrical grabens mostly running in a N-S direction. Analysis of sedimentary facies of the basins' infill supports the simple graben model by revealing lateral alluvial/colluvial fans in basin margins and axial fluvial/lacustrine environments in a central trough. The long-term changes between fluvial and lacustrine conditions in the basins are attributed to paleoclimatic origin. Paleostress analysis of slickensides substantiates that the basins were deformed under E-W extension and related N-S compression in the Late Miocene times, and this stress field would have been started in early Miocene times parallel to the Büyük Menderes Graben (BMG). Following a basin-wide unconformity related to a short-lived compression in mid-Pliocene times, the stress field changed to a N-S extension as a result of the onset of the Büyük Menderes Detachment in the north in the Late Pliocene-Early Quaternary. Emergence of the modern BMG bounded by high-angle normal faults in the north caused a progressive drop of base level and resulted in southward-developing fluvial incision since the Late Quaternary in the studied basins.

Key words: Basin analysis, Büyük Menderes Graben, Karacasu and Bozdoğan grabens, paleostress analyses, West Anatolia

1. Introduction

The E-W–running Büyük Menderes and Gediz grabens, with their prominent morphologies, have attracted the attention of many researchers in the study of the Late Oligocene to Recent extension of West Anatolia. Being symmetric to each other, both zones in the Central Menderes Massif represent narrow intracontinental deformation belts with complex structural history and display multiple basin developments (Figure 1). The Büyük Menderes Graben (BMG) is limited by a regional detachment in the north. The basin is surrounded by the E-W–running Küçük Menderes Graben in the north and by the Muğla-Yatağan Basin and Kale-Tavas Molas Basin in the far south. Four Mio-Pliocene depressions (from west to east, the Çine, Bozdoğan, Karacasu, and Denizli basins) having overall N-S trends are situated just south of the BMG (Figure 1).

Modes of development of variously oriented grabens in this region have received little attention. Although there is a hypothesis called the supradetachment transtensional mechanism (Yılmaz et al., 2000; Çemen et al., 2006; Çiftçi et al., 2011; Gessner et al., 2013), it is not substantiated by considerable structural or depositional field data from N-S running grabens. The previous studies in the BMG and in the vicinity of the BMG revealed a complicated and sometimes conflicting Neogene deformation history. For instance, formation of the Söke Basin in the west tip during the Early to Late Miocene was explained in terms of N-S extension (either detachment or high-angle fault-related) (Sümer et al., 2013). On the other hand, both N-S compression- (Gürer et al., 2009) and N-S extension-related sedimentary basins (Emre and Sözbilir, 1987; Cohen et al., 1995; Bozkurt, 2000) were reported in the central part of the BMG in the Middle and Late Miocene. Further east in the Denizli Basin, the extension direction turns to NNW (or NE and NW) (Kaymakçı, 2005; Koçyiğit, 2005). This brief account suggests that further multidisciplinary detailed studies are still required in unexplored areas in order to reconcile or negate the existing conflicting views and provide more detailed structural history in the BMG and its vicinity.

In this study we focused on the stratigraphic, sedimentological, and structural characteristics of the Karacasu and Bozdoğan (K&B) basins just south of the

* Correspondence: focak@ogu.edu.tr

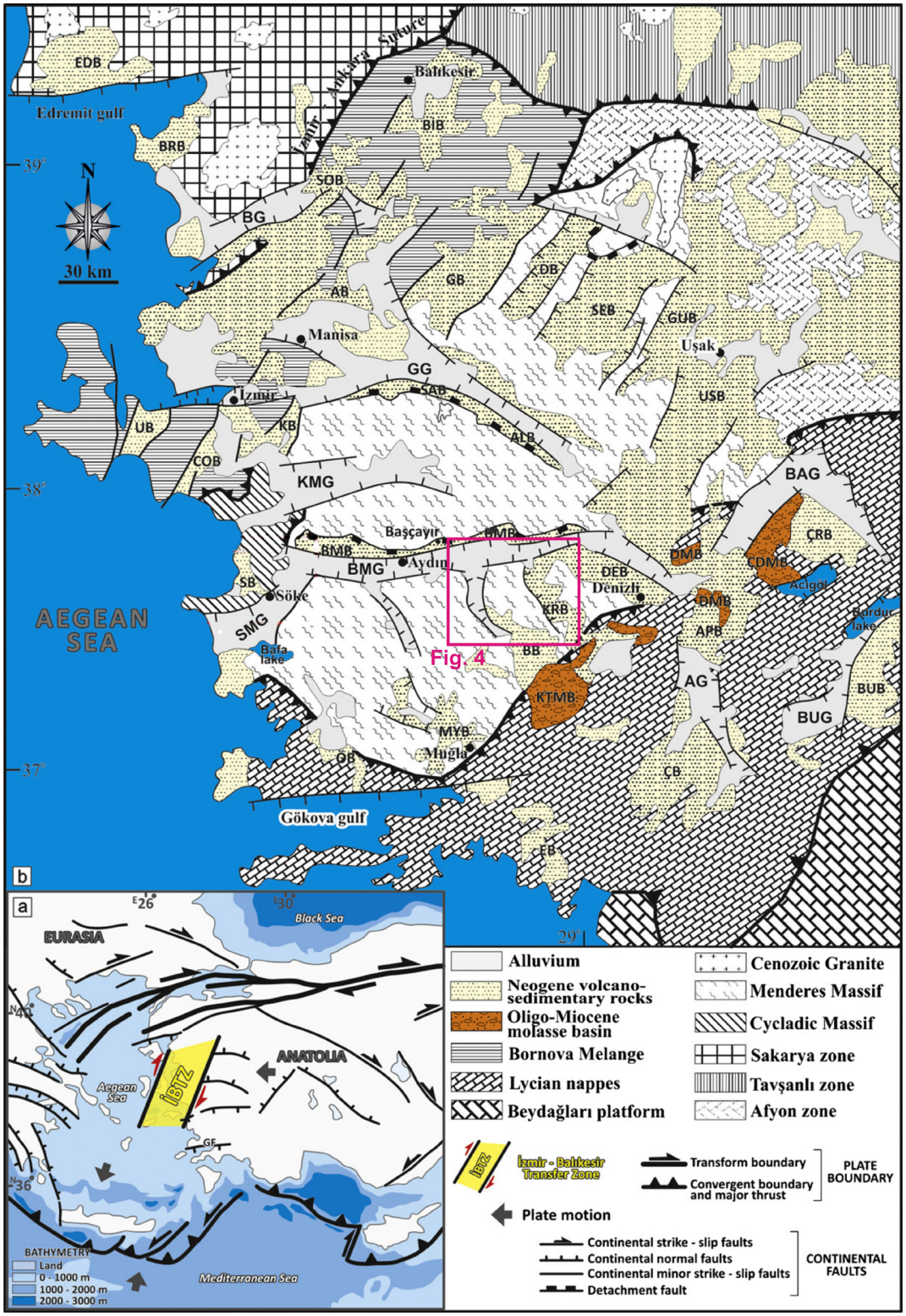


Figure 1. Simplified tectonic map (a) and geological map (b) of western Turkey (after Sümer et al., 2013). AG: Acıpayam Graben, BG: Bakırçay Graben, BAG: Baklan Graben, BMG: Büyük Menderes Graben, BUG: Burdur Graben, GG: Gediz Graben, KMG: Küçük Menderes Graben, SMG: Söke-Milet Graben, AB: Akhisar Basin, ALB: Alaşehir Basin, APB: Acıpayam Basin, BB: Bozdoğan Basin, BİG: Bigadiç Basin, BMB: Büyük Menderes Basin, BRB: Bergama Basin, COB: Cumaovası Basin, ÇB: Çameli Basin, ÇRB: Çardak Basin, DB: Demirci Basin, DEB: Denizli Basin, EB: Eşen Basin, EDB: Edremit Basin, GB: Gördes Basin, GUB: Güre Basin, KB: Kocaçay Basin, KRB: Karacasu Basin, MB: Muğla-Yatağan Basin, ÖB: Ören Basin, SAB: Salihli Basin, SB: Söke Basin, SED: Selendi Basin, SOB: Soma Basin, UB: Urla Basin, USB: Uşak Basin, ÇDMB: Çardak-Dazkırı Molasse Basin, DMB: Denizli Molasse Basin; and KTMB, Kale-Tavas Mollase Basin.

BMG (Figure 1). Our aim is to reveal the depositional and structural history of these basins and to discuss their significance in the context of the Central Menderes Massif and the broader area of West Anatolia.

The Karacasu graben has been recently studied in terms of basinfill pattern and its paleoclimatic relevance (Ocakoğlu et al., 2007; Alçiçek and Mayda, 2009; Alçiçek and Jimenez-Moreno, 2013). However, studies concerning the structural evolution of both grabens, particularly recognition of structural controls in the basinfill, are scarce or unpublished (Paton, 1992; Ocakoğlu et al., 2007). The present study serves to draw a more complete spatiotemporal tectonosedimentary picture of Neogene extension in the vicinity of the BMG by filling in the existing gaps.

2. Geometry of the studied basins

The K&B basins have distinct overall morphological and basement topographical features beneath the Mio-Pliocene infill. These features can be viewed as fundamental clues for determining the deformation during and after basin formation (Figures 1 and 2). Here we begin with the prominent morphological features of the horsts and grabens (from the West to East Madran horst, Bozdoğan graben, Karıncalıdağ horst, Karacasu graben, Babadağ horst, and eastern Denizli graben in Figure 2). Next, the basement topography was indicated by electrical resistivity data. These data were collected and interpreted by Yıldız et al. (1986). We georeferenced them and checked with available drillhole data in the grabens.

The most prominent morphological attribute of the studied grabens is their slightly curved plan view (Figures 1 and 2a). The basin axes are nearly N-S–oriented near the BMG and are increasingly deflected E-W in the south (Figure 2). Moreover, a progressive deviation of the northernmost borders from NS to NW was distinguished from the Bozdoğan graben to the Denizli graben. A second common feature of the grabens is the presence of noticeable scarps at their NW margins and near the BMG (Figure 2a). Three profiles running NW through the horst ridges and another profile traversing the studied grabens from the NE provide additional morphological information. The Madran profile (A-A' in Figure 2b) shows a highly dissected rounded morphology at approximately 1400 m. Regarding the Karıncalıdağ case, a dissected plateau is evident at the same altitude. In contrast with the Babadağ horst, the higher plateau dips slightly NW and the elevation gradually decreases from 2000 to 1400 m (C-C' in Figure 2b). All of the NW profiles through the horst crests demonstrate a sharp break as they approach the southern margin of the BMG. In the E-W profile (D-D' in Figure 2b), 2 points are notable. First, the horst crests always extend 1500 m (slightly more in the Madran horst). In addition, the horst crests are asymmetrical (i.e. steeper on the eastern margins and less steep on the western margins). Furthermore, an unequivocal profile break was observed at 100 m on the eastern margin of each of the studied grabens (Figure 2b). This observation will be discussed later.

The geomorphology of the interior of the K&B basins displays considerable variation. The Bozdoğan graben is deeply dissected by the Akçay creek to form a broad valley at about 50–90 m above sea level where a thin veneer of fluvial sediments was deposited. A widespread depositional surface belonging to the uppermost level of Mio-Pliocene basinfill (MUS in Figure 2a) is still remarkable to the east of Yenice at 700–800 m (E-E' in Figure 2b). In the Karacasu graben, fluvial incision gradually decreases from the north to the town of Karacasu. In the vicinity of Karacasu depositional surfaces of coalesced alluvial fans (KYK in Figure 2a) at 500–600 m are still being rapidly eroded by tributaries of the Dandalas creek. To the east of the village of Geyre the incision wanes out. Considerable Late Holocene alluvial sedimentation was reported over the ancient city of Aphrodisias further east of Geyre (Ratte, 2001).

The basement topographic traits of the studied grabens are very similar (Figure 3). Both grabens have a central trough that runs approximately N-S. The central troughs are cut by N-W to E-W running lineaments in the south (Figure 3). In both cases, the central depressions are symmetrical with maximum basement depths of –300 m. The Karacasu graben basin floor suddenly dips northward in the northwest near the BMG. This trend is not observed in the neighboring Bozdoğan graben (Figure 3). In addition, the available data indicate the presence of buried faults. These faults and this basin margin morphology are generally conformable in the Karacasu graben but are discordant south of the Bozdoğan graben (Figure 3).

3. Stratigraphy

The oldest Menderes massif rocks on the horsts are Precambrian migmatite and gneiss, which are overlain by Paleozoic marble and quartz-schist towards their periphery (Konak and Göktaş, 2004). The upper part of this succession is represented by Mesozoic marble and schist (anonymously known as "cover series"), which have progressively lower grades of metamorphic features upward (Figures 4 and 5) (Bozkurt and Oberhansli, 2001). Here, Cretaceous ultramafic rocks (mainly peridotites) tectonically juxtapose the cover series on the southeastern tip of the Karacasu graben (Candan et al., 2000) (Figure 5). The boundaries between certain metamorphic rocks and foliation planes dominantly occur from N to NE-SE of the Madran and Karıncalıdağ horst. However, no preferred foliation is apparent in the Babadağ horst (Konak and Göktaş, 2004).

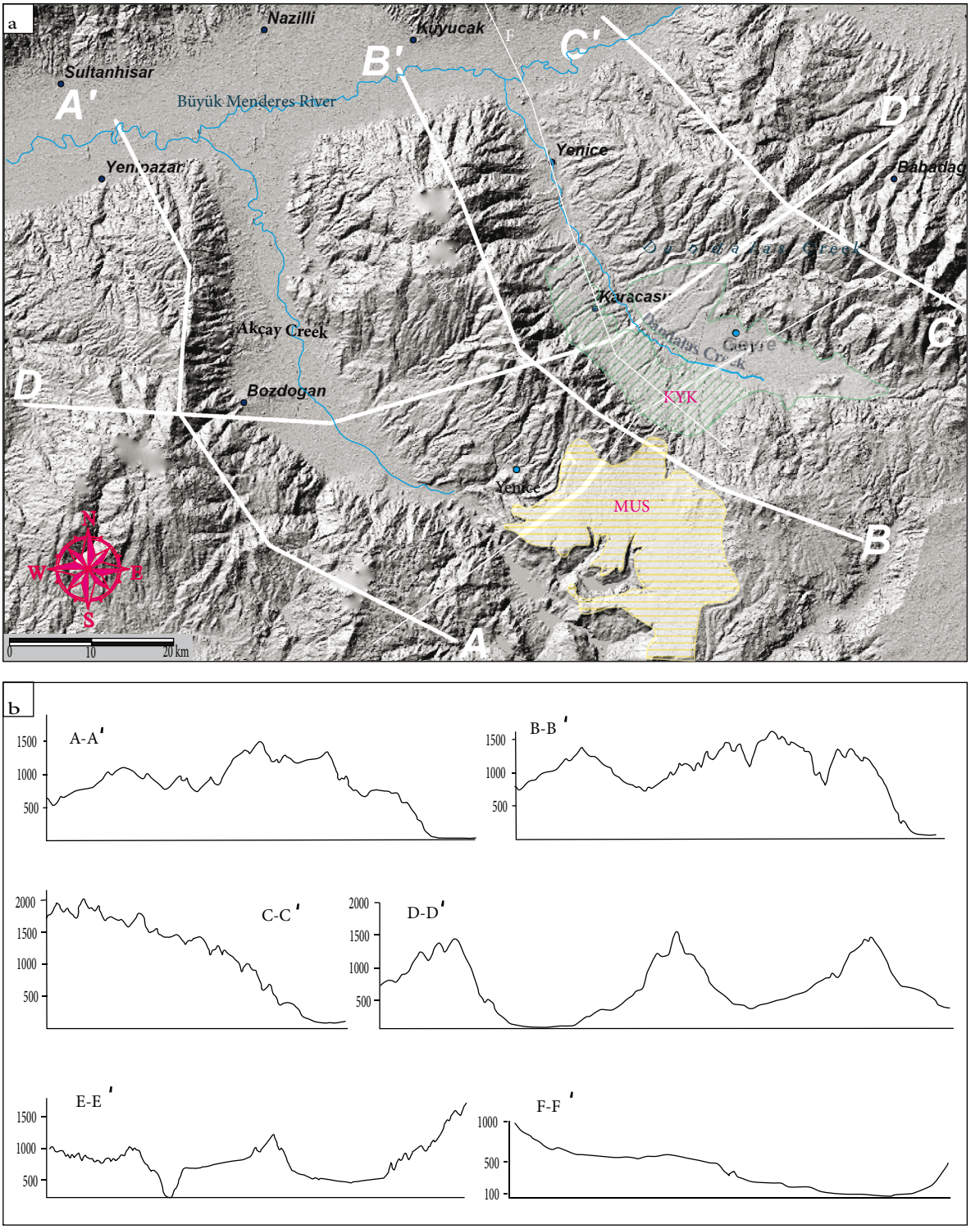


Figure 2. (a) DEM view (Aster data) and (b) topographic profiles across the Karacasu and Bozdoğan grabens.

Cenozoic infill of both grabens was stratigraphically investigated by many researchers (Nebert, 1955; Becker-Platen, 1971; Kastelli, 1972; Açıkalın, 2005; Alçiçek and Jimenez-Moreno, 2013). Correlation with other West Anatolian basins was also carried out (Becker-Platen, 1971; Alçiçek, 2010). Here we adopted the lithostratigraphic nomenclature proposed by Açıkalın (2005) in the Karacasu basin, which consists of 2 lithostratigraphic

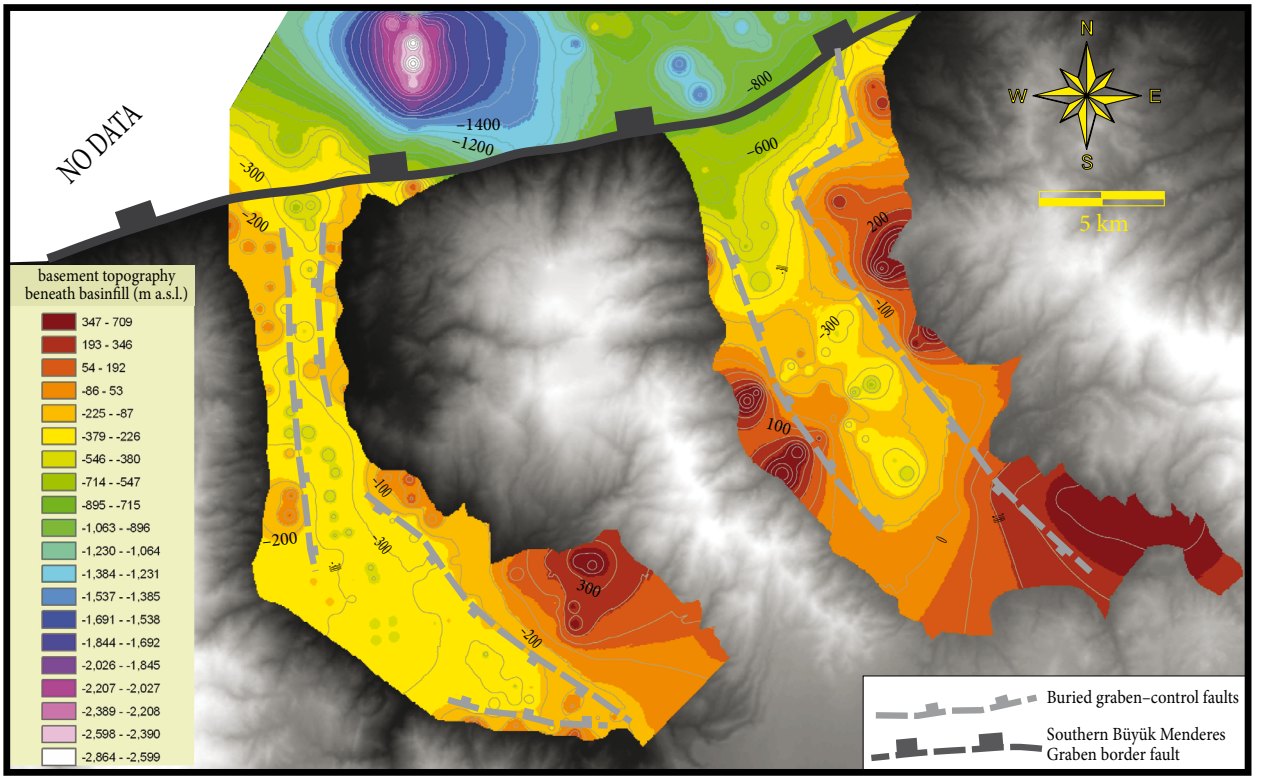


Figure 3. Basement topography based on electrical resistivity data (Yıldız et al., 1986) in the Karacasu and Bozdoğan grabens and in the northern vicinity.

units separated by an unconformity (Figure 4). The lower unit, called the Dandalas group, comprises 2 interfingering formations. The Damdere formation extensively crops out across the eastern margin of the Karacasu graben in the vicinity of the villages of Işıklar, Damdere, and Karacaören, and it consists of reddish conglomerate and sandstone that fill the isolated paleovalleys (Figure 5). In the graben interior, it is a yellow-colored, well-organized sandstone-conglomerate alternation with considerable fines, and it forms the uppermost stratigraphic levels of the Mio-Pliocene basinfill south of Karacasu. In the Bozdoğan graben, the Damdere formation mostly occurs across the eastern margin around Olukbaşı and Yenice villages and has almost identical lithologic features to those of the Karacasu graben (Figure 5). The outcrops around Güvenir further south are overlain by the Karacaören formation.

The Karacaören formation typically consists of gray to white mudstone-limestone alternations with significant intercalation of sandstone, gypsum, dolomite, and organic-rich intervals. The unit locally includes a rich diatom and ostracod fauna (Açıkalın, 2005; Alçiçek and Jimenez-Moreno, 2013). Separate mudstone- and limestone-dominated intervals are recognized in the unit by this study and by Alçiçek and Jimenez-Moreno (2013).

The estimated maximum thickness of the Dandalas group in the Bozdoğan graben is 1100 m based on the elevation of the basement beneath the basins (–300 m) and the uppermost depositional surface of the unit (800 m).

All reliable age data come from the Bozdoğan graben. They are based on mammalian fossils and vary from Tortonian (MN9) to Messinian (MN13) (Table 1). The Berdik-1 mammalian site 7 km SE of the village of Güvenir in Figure 5 indicates a slightly older age (Late Middle Miocene, MN7) (Şen and Sarıca, 2011; Table 1). Age constraints in the Karacasu graben are rather weak and indicate the Early Pliocene for the Karacaören formation based on Ostracoda fauna (Kastelli, 1972) and also the pollen assemblage (Benda and Meulenkamp, 1990).

The Karacasu formation unconformably overlies the Dandalas group (Figures 4 and 5). This unit consists of gravelly sandstones and boulder conglomerates that become redder towards the surface. The contact relationship is mainly obscure in the basin margins where the incision is limited and where juxtaposition occurs between the 2 continental units. Towards the basin center, particularly in the Karacasu graben, the Karacasu formation rapidly advances towards the basin over the already deformed Karacaören formation. In addition, reworked lacustrine materials mainly occur beneath the Karacasu formation (Ocakoğlu et al., 2007). A basal unconformity widely occurs at 400 m a.s.l. in the Karacasu graben. A mammalian fossil site (F5 in Figure 5) found southeast of Karacasu by

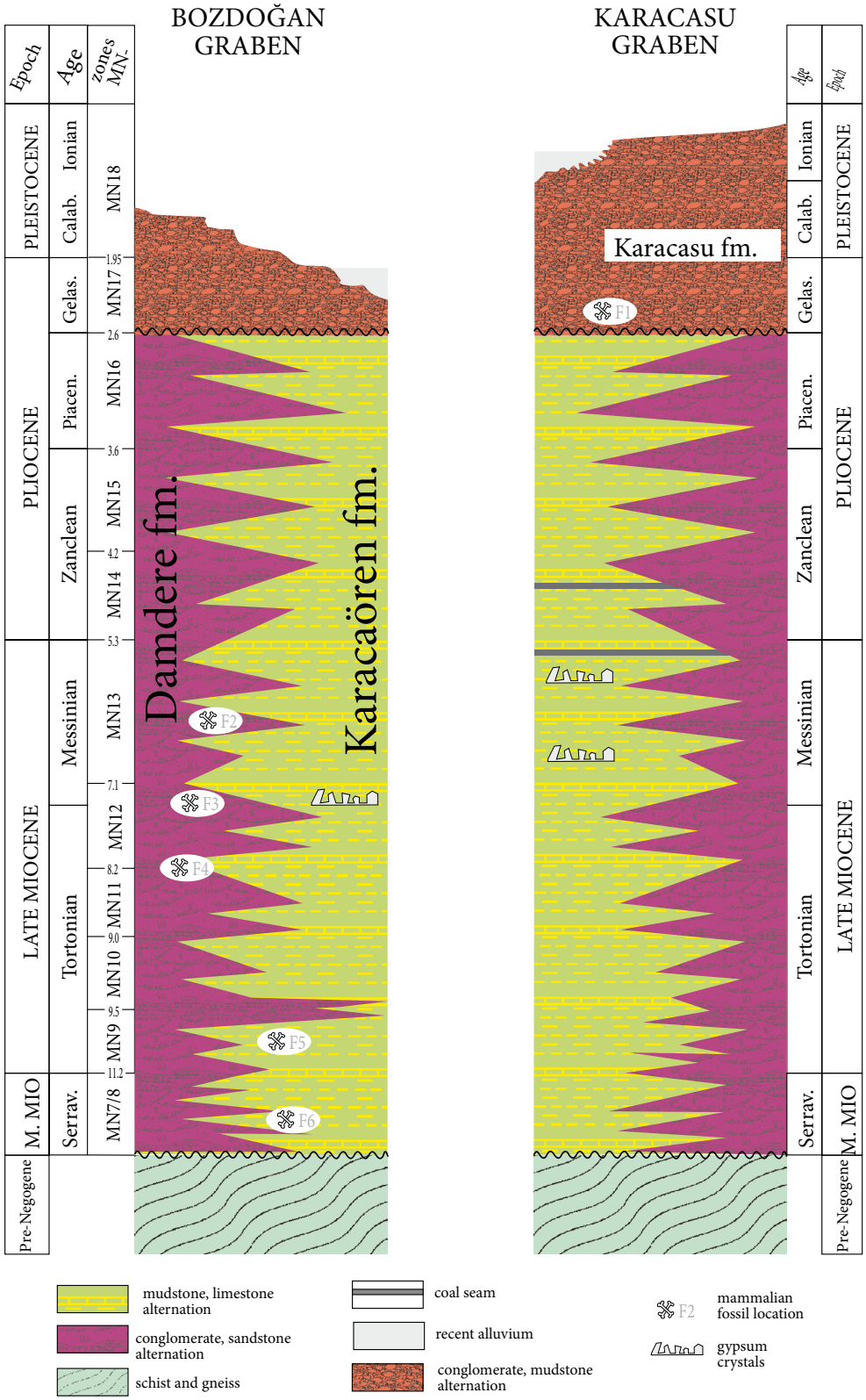


Figure 4. Generalized stratigraphic columns of the Karacasu and Bozdoğan grabens. Mammalian fossil locations. F1 to F6 are explained in Table 1.

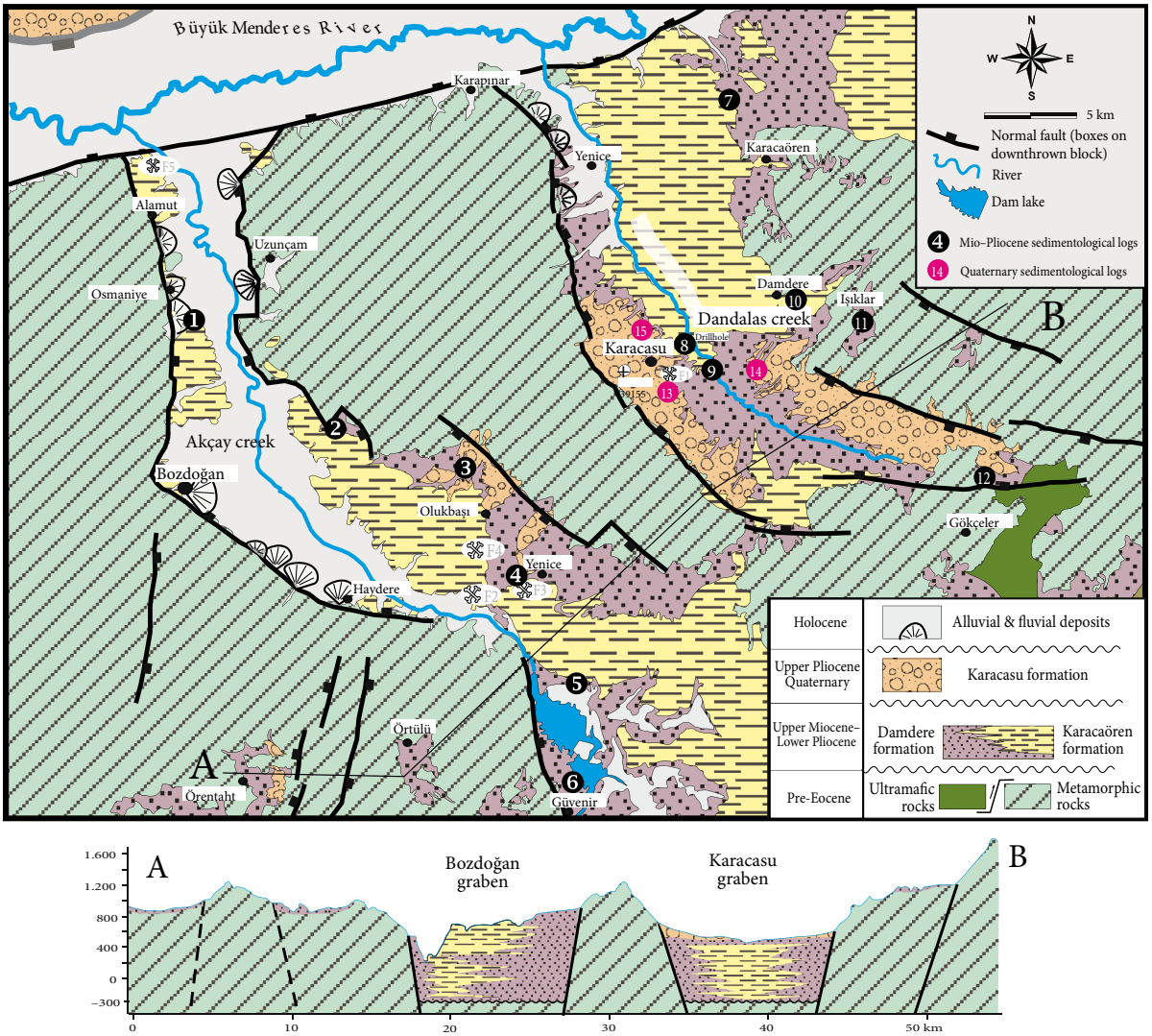


Figure 5. (a) Geological map of the Karacasu and Bozdoğan grabens area (revised from Konak and Göktaş, 2004). (b) A-B geological cross-section.

Açıkalın (2005) indicated the presence of an MN17 zone in the lowest part of the Karacasu formation (F1 in Table 1). The uppermost level of the Karacasu formation is well preserved as a planar geomorphic surface in the Karacasu graben at altitudes of 700–750 m (KYK in Figure 2).

The youngest stratigraphic unit only occurs in the low-lying plains that border the western margins of the depressions. Significant spatiotemporal differences were observed between the 2 grabens (Figures 4 and 5). In the Karacasu graben, these modern deposits unconformably overlay the older rocks and geographically extend upstream near Yenice 10 km from the northern outlet of the graben (Figure 5). Within this mostly geomorphic unit, an alluvial terrace and an actively developing alluvial fan complex were distinguished at 300 and 190 m, respectively (Ocakoğlu et al., 2005). In the Bozdoğan graben, the youngest unit is more widespread but patchy east of the Haydere village and 35 km upstream from the northern graben outlet (Figure 5). Here, one can distinguish at least 5-km-sized alluvial fans in the north with apexes of 170–190 m (some of these alluvial fans are already under incision). Three distinct alluvial fan terraces in the vicinity of the Osmaniye town (apex between 290 and 180 m) should belong to this unit (Figure 5). Towards the basin center, the axial braided Akçay creek deposits coarse sands and gravel on the graben floor.

4. Sedimentology of the graben fill

4.1. Miocene-Early Pliocene infill (Dandalas group)

A total of 11 sedimentological logs, 6 from the Bozdoğan graben and 5 from the Karacasu graben, were measured to understand the depositional conditions based on

Table 1. Mammalian finds from the Bozdoğan and Karacasu grabens.

Location no.	Mammalian fauna	Mammal zone	Location and reference
F1	*Equus stenonis*, *Bos* sp.	MN17	Karacasu Açıkalın (2005)
F2	*Adcrocuta eximia*, *Tetralophodon grandincisivus*, *Hipparion* sp., *Chilotherium schlosseri* and *Ceretotherium neumayri, Schizogalerix* n. sp., *Desmanella amasyae*, *Amblycoptus* sp. and Soricidae indet. *Parapodemus gaudryi*, *Apodemus gudrunae*, *Hansdebruijnia neutrum*, Muridae n. gen. n. sp., *Byzantinia uenayae*, *Hypsocricetus strimonis*, Cricetidae indet., *Pseudomeriones* sp.	MN13	Amasya Sickenberg et al. (1975) Schmidt-Kittler (1976) Gaziry (1976) Staesche and Sondaar (1979) Engesser (1980)
F3	Cricetinae, Cricetodontinae, *Byzantinia uenaye*, *Ochotonidae prolagus*	MN12	Amasya-1 Saraç (2003)
F4	*Hipparion*, *Ceratotherium neumayri*	MN11-12	Olukbaşı Saraç (2003)
F5	*Byzantinia* aff. *dardanellensis, Byzantinia* n. sp., *Megacricetodon debruijni*, Cricetidae indet. *Myocricetodon eskihisarensis*, *Sinapospalax* sp., *Myomimus dehmi*, *Microdyromys* sp., Gliridae indet., *Lophocricetus* sp.	MN9	Direcik Sarıca-Filoreau (2002)
F6	*Desmanella* sp., *Desmanodon* cf. *minor*, *Alloptox* cf. *gobiensis*, *Keramidomys* sp., *Myomimus* sp., *Cricetodon candirensis*, *Megacricetodon* aff. *similis*, *Democricetodon brevis*, *D. freisingensis*, *Gomphotherium* sp., *Cricetodon candirensis*	MN7	Berdik-1 Sickenberg et al (1975) Sarıca-Filoreau (2002)

basin evolution. In addition, data from one drillhole (Dağ, 1990) in the Karacasu graben were included. When possible, logging sites were selected based on their representativeness and vertical rock continuity. Because the modern morphology of the grabens mainly mimics the original shape and the relict basinfill mainly outcrops at the eastern margins of the basins, the sedimentological logs were retrieved in a shifting manner towards the basin margins. Thus, the superposition of the sedimentological logs should not be considered as pure vertical stacking because it includes a lateral transition.

Based on lithology, sedimentary structure and texture, color, geometry, and fossil content, we distinguished 16 distinct sedimentary facies along the sedimentological logs. Each facies is interpreted in terms of specific hydrodynamic/chemical conditions and related with similar examples in the literature (Table 2). Regarding close relation and affinity between the facies, we regrouped them into 3 facies associations and 6 facies subassociations (Table 3). They are all terrestrial in nature and range from proximal alluvial fan to deep alkaline lake environment. In the following subsections we address the distributions of facies associations/subassociations with special reference to distinct sedimentary facies in order to figure out the infill architecture of each graben.

4.1.1. Bozdoğan graben

Sedimentological logs from this graben come rather from the basin margin except for the Yenice and Baraj-2 logs, since the Akçay creek mostly eroded basinal sediments in the Quaternary (Figure 5). Sedimentological logs are 75 to 430 m thick and represent the upper half of a presumably 1100-m-thick basinfill (see Section 2).

The graben infill consists of 2 dominantly lacustrine sedimentary packages (hereafter the lower and upper packages) separated by a fluvial intertongue of 35–55 m in thickness (Figure 6). The lower lacustrine package laterally passes to subaerial facies associations in the northern sedimentological logs (Kavaklı, Gedikağzı, and Olukbaşı), but it basically consists of the lacustrine subassociation of LFA1 and LFA3 in the south. The Olukbaşı log on a probable basement uplift in the northern basin margin is made from the alternation of Bc and Gc facies to form the 15-m-thick Alluvial Fan Association (AFA). Here the facies Bc is formed from the angular monogenic gravels in a sandy mud matrix, and it quickly grades laterally to gravelly sand facies (Sm) within tens of meters. The interbedded Gc facies (Figure 7a) with imbricated large (max. 30 cm) blocks indicates paleoflow towards the south. This facies association displays lateral passage to massive clast-supported and cross-bedded conglomerates

Table 2. Description and interpretation of facies observed in the infill of grabens.

Facies and description	Process/subenvironment
Clast-supported conglomerate (Gc): Polygenic gravels, angular to subangular, up to 20 cm in size. Clast-supported texture with frequent imbrication of oval clast (Figure 7a). Poor to moderately sorted. Coarse sand to granule matrix. Massive, but rarely displays crude bedding. 1–4 m thick individual beds. Erosional lower contact and rapid pinch-out in several to tens of meters. Frequently overlain by facies Sm, Gp, and Gt.	Subaerial fluid flow concentrated in channels (Miall, 1977, 1978; Rust, 1978)
Planar cross-stratified conglomerate (Gp): Clast-supported, inclined (10–20°) gravel bed sets of up to 1 m thick. Complex intertonguing with pebbly sand layers. Subrounded polygenic gravels with some intraformational mud clasts. Limited lateral extend only several tens of meters. Irregular erosive lower contact. Complex intertonguing laterally and vertically with facies Gm and Sh.	Fluid flow on longitudinal and point bars (Miall, 1977; Rust, 1984; Bluck, 1986)
Trough cross-bedded conglomerate (Gt): Clast-supported gravels with dm to m-size trough cross-beds with thickness of <1 m. Lower contact displays shallow erosion. Laterally continuous for several meters, passing to facies Gm and Gp.	Flow erosion and fill in secondary channels (Miall, 1978; Rust, 1978)
Matrix-supported conglomerate (Gms): Yellow to red coarse sand to mud matrix enveloping randomly distributed angular clasts (Figure 7b). Larger clasts locally concentrate at the top of bed. Internally massive, bed thickness rarely exceeds 2 m. Lobate in shape, termination within tens of meters laterally. Rarely passes gradationally upward to facies Gm, Gp.	Subaerial cohesive debris flow (Miall, 1978; Nemec and Postma, 1993)
Clast-supported Breccia (Bc): Very angular, monogenic, large clasts (5–30 cm) come together with a massive clast-supported texture. Intergranular space filled with sandy mud. Laterally passes to gravely sands in tens of meters. Occurs at or close to basal unconformity, alternates with facies Gm.	Rockfall and grain flows on steep colluvial surface (Nemec and Steel, 1984; Blikra and Nemec, 1993)
Clast-supported bedded gray conglomerates (Gs): Gray to green stiff conglomerate having very angular clasts in contact with each other. Intergranular space fills with moderately sorted sand. Basal contact of individual beds displays rarely low-angle truncations, but rather nonerosional. Displays complex intertonguing and alternation with gravelly sands (facies Sms) in tens of meters downslope. Bed thickness of <1 m.	Subaqueous grain flows (Hwang and Chough, 1990; Hwang et al., 1995)
Massive gray (gravelly) sandstone (Sms): Massive, rarely parallel-bedded, nonerosional based gray-green sandstone with gravel trains and lenses. Thickness of beds is about 1 m, rarely exceeding 2 m. Grain size considerably decreases to fine sand within 50 m downslope. Basal contact is gradational on facies Gs. Ball-and-pillow structure occurs locally.	Subaqueous sandy grain flow (Hwang et al., 1995; Kim et al., 1995)
Massive (gravelly) red sandstone (Sm): Brick-red to yellow, massive, poorly sorted, laterally extending tens of meters. Locally comprises gravels trains and thin lenses. At uppermost levels, poor paleosol development (facies P). Mostly <1-m-thick beds, but may be as thick as 4 m. Internally parallel bedding and reactivation surfaces occur. Most frequently overlies the facies Gm.	Deposition from heavily sediment-laden flows from waning floods (Miall, 1977, 1978; Todd, 1989)
Planar cross-stratified sandstone (Sp): Green- to yellow-colored, medium sorted sandstone with occasional larger rip-up clasts. Basal contact erosive, and reactivation surfaces may occur between cross-bed sets. Cross-bed height up to 50 cm. Amalgamated cross-bed sets reach 3 m thick. Laterally extensive for several 100 m. Frequently overlain by facies Fl.	2D dunes, linguoid bars (Miall, 1978, Harms et al., 1982)
Massive to cross-bedded fossiliferous sandstone (Smf): Gray- to yellow-colored, fine to coarse sandstone. Considerable lateral extend (hundreds of meters), gradual contact with underlying/overlying marly facies. Internally massive or diffuse even bedding. Locally abundant macrophyte debris and bivalve, Ostracoda, and diatom fossils (Figure 7c). Symmetrical ripples, and *Ophiomorpha* and *Skolithos* trace fossils occur locally when coarser-grained.	Traction to suspension siliciclastic deposition in littoral lake (Valero-Garcés et al., 2014)

Table 2. (continued).

Laminated silt/mudstone alternation (Fl): Color ranges red to green. Thickness of siltstone <10 cm, displays poor soil development at top (Figures 7d and 7e). Root casts and mottling common. Mudstone is massive and hosts nodular to banded caliche formation. Thickness of facies interrupted by facies Sp and Gp is 1–4 m. Laterally continuous for several hundreds of meters.	Suspension settling from flood waters and later modification by pedogenesis (Miall, 1977, 1978; Bentham et al., 1993; Kraus, 1999)
Massive gray marl (Fmm): Color ranges from green to whitish according to carbonate and diatom content. Locally lamination may be preserved, but generally massive due to intense bioturbation. Randomly disseminated silica and carbonate nodules up to 20 cm, and massive sulfur enrichments in small paths (3–5 cm) in the facies (Figure 7f). Individual thicker beds up to 10 m are traced for many hundreds of meters. Frequently alternate with micritic limestone facies (Lm) on cm to m scale.	Suspension settling in relatively deep lake setting and subsequent bioturbation and diagenetic changes (Cohen, 2003; Valero-Garcés et al., 2014)
Black shale (Fbs): Dark gray to black, laminated, laterally extensive mudstone for many hundreds of meters. Individual beds 5–60 cm. Frequently alternate with gray marl (Fmm) and micritic limestone (Lm) (Figure 7g).	Suspension deposition in deep anoxic lake (Barnes and Barnes, 1978; Cohen, 2003)
Micritic limestone (Lm): White- to cream-colored, cm- to 3-m-thick beds. Thinner beds display stromatolitic lamination and tepee structures locally. Thicker beds are massive due to intense bioturbation. A rich mollusk and Ostracoda fauna occurs in the facies. Even finer beds can be traced for several hundreds of meters laterally. Frequently alternate with black shale (Fbs) and gray marl (Fmm) facies with gradational contacts.	Carbonate deposition in littoral to sublittoral alkali lake (Dean and Fouch, 1983; Platt and Wright, 1991; Cohen, 2003)
Gypsum (G): Found as thin (<5 cm) powder-like or crystalline beds, or disseminated larger (2–3 cm) euhedral crystals in gray marl facies of up to 30 cm thick (Figure 7e). Individual gypsiferous levels are discontinuous, traced only for tens of meters. Lateral and vertical gradation to gray marl (Fmm) and massive sand (Smf) facies.	Evaporation in lake margin mudflats and pools, and subsequent early diagenetic crystallization (Warren, 2006; Schreiber and El Tabakh, 2000)
Paleosol (P): Massive mud with some floating cm-sized host rock/sediment clasts. Color ranges from yellow to brown/red. Rubification at the top is typical. Columnar structure is common. Caliche nodules and bands up to 5–10 cm are also developed (Figure 7d). Locally root traces and charcoal are distinguished. Thickness is 5–150 cm, lateral continuity is about tens of meters.	Chemical alteration and physical deformation of existing material (Lechman, 1989; Retallack, 2001)

Table 3. Organization of facies into facies associations and facies subassociations in the studied graben fills.

Facies association	**Incorporating facies**
Alluvial Fan Facies Association (AFA)	Gc, Gms, Gcb, Sm, lesser P
Fluvial Facies Association (Facies Association) (FFA)	
• Low-sinuosity subassociation (FFA1)	Gc, Gp, Gt, Sp, lesser Fl, P
• High-sinuosity subassociation (FFA2)	Gp, Gt, Sp, Fl, P
Lacustrine Facies Association (LFA)	
• Fan-delta subassociation (LFA1)	Gs, Sms, lesser Fmm
• Litoral siliciclastic lake subassociation (LFA2)	Smf, lesser Lm
• Shallow carbonate/evaporite lake subassociation (LFA3)	Lm, J, lesser Fmm
• Deep alcaline lake subassociation (LFA4)	Fmm, Fbs, thin Lm

(Facies Gc and Gp) and thin massive sandstone (Sm) that together form the FFA1 subassociation. The correlative of this subassociation in the Kavaklı log in the north is represented by a rather sandy facies. The lower part of the log (0–49 m) is dominantly formed by massive to locally cross-bedded sandstone (Facies Sm). Thin paleosol levels

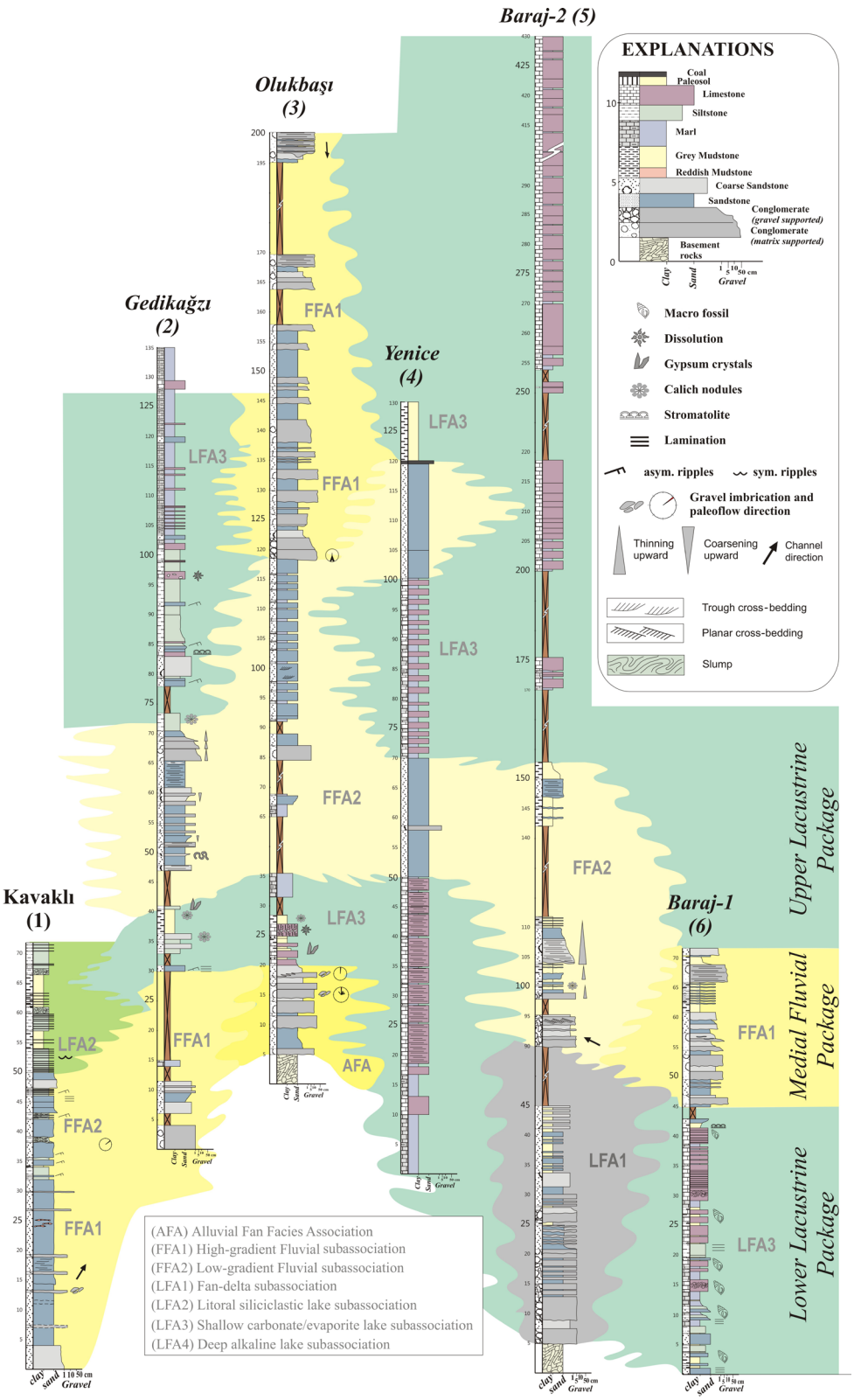


Figure 6. Measured sections from the Bozdoğan graben (see Figure 5 for locations of logs).

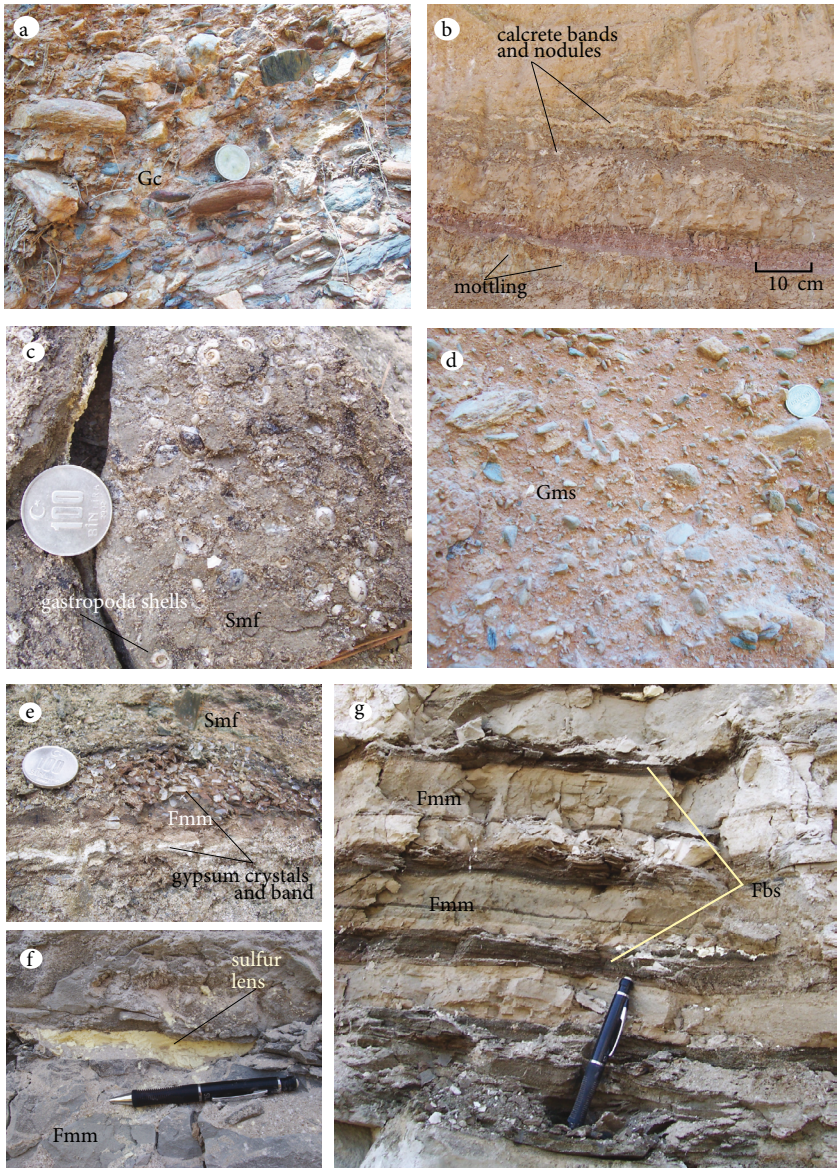


Figure 7. Sedimentary facies from the studied grabens. (a) Clast-supported conglomerates from Damdere log. Note imbrications of gravels in horizontal bed. (b) Fl facies with poorly developed paleosol including calcrete nodules and bands (Baraj-2 section). Poorly sorted clasts are mostly angular. (c) Massive sandstone facies with plenty of Gastropoda shells. (d) Matrix-supported conglomerates in Işıklar log. (e) Gypsum facies (banded fine crystals and euhedral large crystals) developed in fine sandstone and mudstone (Dandalas section). (f) large native sulfur lens developed in Fmm facies (Dandalas log). (g) Alternation of Fmm and Fbs (black shale) facies in Karacaören log.

(Facies P) and occasional erosive-based conglomerates with angular components (Facies Gc) are also observed. Channel directions and gravel imbrications indicate NE-directed paleocurrent. Upwards in the section, cross-bedded sandstone and siltstone (Sp, St) alternate with considerable fines (Facies Fl).

The lower lacustrine package in the Baraj-2 section starts with the Fan-Delta subassociation (LFA1) (Figure 6). It is basically composed of 2 facies (Gs and Sms) with complex vertical and lateral gradation. Both facies laterally pass to a shallow carbonate lake subassociation (LFA3) in the neighboring sections. Lm, Fmm, and thin Fbs facies alternate in dm- to m-scale. Mollusk and Ostracoda fossils are locally abundant. Several m-thick slumps in thin-bedded Lm facies are also present in the Baraj-1 section (Figure 6). In the Gedikağzı and Olukbaşı sections in the

NW several calcrete and gypsum levels (facies P and G) occur in the same stratigraphic level.

The medial fluvial package belongs to a low-gradient fluvial subassociation (FFA2), except for the Baraj-1 section. It is characterized by the occurrence of the facies Gc, Gt, Sm, Sp, and Fl and the poorly to moderately developed P facies, which together form fining-upward cycles of 2–5 m in thickness. Erosive bases, intraformational lag gravels, red-colored locally mottled mudstone, and calcrete bands and nodules are the most frequent features in the cycles (Figure 7b). Planar cross-bed measurements verify the NW-running axial fluvial current in the Baraj-2 section (Figure 6).

The upper lacustrine package is mostly built from the Shallow Carbonate/Evaporate Lake subassociation (LFA3) with considerable interfingering of the High-Gradient Fluvial subassociation (FFA1) around the Olukbaşı section (Figure 6). The contribution of Fmm, Lm, and thinner Smf facies (Figure 7c) in the subassociation considerably varies with respect to position of sections. White to gray marl is thicker (2–3 m) in the Gedikağzı log but quite thinner (<20 cm) in the Baraj-2 and Yenice logs. The opposite applies to facies Lm. This latter is generally laterally continuous for several hundreds of meters in thicker beds. The interfingering fluvial subassociations in the vicinity of the Oluklu section are made from sandy facies (Sp, St, and, to a lesser extent, Fl) at the base (80–120 m) and became coarser upwards (35 cm in size) (Figure 6). Three facies (Gc, Sm, St) made the bulk of the FFA1, forming fining-upward cycles of 3–5 m thick. Clast imbrications and channel directions indicate south-directed paleoflows (Figure 6).

4.1.2. Karacasu graben

Sedimentological logs from the Karacasu graben are thinner (80–220 m) compared to the Bozdoğan graben due to lesser Quaternary incision in the former (Figure 8).

The lowermost stratigraphic intervals belong to subaerial associations (AFA and FFA1) in the SE sections, which were uplifted by presumably dip-slip faults (Figure 5). These deposits fill the kilometer-wide paleovalleys in Işıklar and Damdere villages (Ocakoğlu et al., 2007) and are composed of gravelly and sandy facies. Massive, matrix-supported red conglomerate (Gms) is the dominant facies in the Işıklar log (Table 2; Figure 7d). It is laterally discontinuous and would display reverse grading. Clast-supported massive conglomerate (Gc) and red massive sandstone (Sm) are also frequent. In the Damdere section, the size of clasts is smaller. Erosive-based Gc facies is overlain by massive red pebbly sandstone and poorly developed paleosol to form cycles of 3–5 m thick. Facies Gms is almost absent, probably due to more distal alluvial setting. An overall fining-upward trend is also evident up to 55 m. Clast imbrication from the Damdere log indicates paleoflow towards the SW, which is in accordance with paleovalley orientation. Both sections are ascribed to the AFA association. The AFA association laterally passes to a low gradient subassociation (FFA2) towards the SE in the Kızılbayır section (Figure 8). Alternation of the facies Gm, Sm, Fl, and P occurs here. Muddy and paleosol intervals form almost half of the section. A thick paleosol interval of up to 3 m thick is developed on top of the ultramafic basement and sandy facies (Sm) as well. It is frequently accompanied by nodular to banded calcrete. Clast imbrications in conglomerates indicate paleoflows from the NNW and NNE (Figure 8).

The overlying lacustrine sediments start with the Shallow Carbonate/Evaporate Lake subassociation (LFA3) and evolves to a Deep Alkaline Lake subassociation (LFA4). The ensuing shoaling later gives way to LFA3 and then the Littoral Siliciclastic Lake subassociation (LFA2) (Figure 8). The lower LFA3 subassociation is about 100 m thick. It is composed of thin Lm and massive, thick Fmm alternation in the basin margin (Damdere log). In the Dandalas and Karacaören logs, Fmm is fossiliferous (mollusks and Ostracoda) and massive to laminated, and alternates with thin Lm and G facies. Facies G is less than 50 cm thick and developed as large euhedral crystals in Fmm (Figure 7e). Frequent gypsum crystals were reported in the drillhole in this facies subassociation (Figure 8). We defined a thin (4–5 m) clastic unit belonging to LFA2 in this subassociation (Figure 8). It would be correlative all over the basin and is composed of fossiliferous Smf and Fmm alternations with native sulfur nodules and lenses (Figure 7f). The overlying LFA4 subassociation is thickest (150 m) in the Karacaören section and rapidly thins out towards the basin margin (Figure 8). Alternation of different Fmm facies with apparently varying carbonate content (from mudstone to marl) forms the bulk of the subassociation. Thin (<10 cm) Lm and Fbs facies would be interleaved (Figure 7g). Carbonate and siliceous nodules and lenses up to 20 cm in size are frequent all over the subassociation. The LFA3 subassociation further above is characterized by the increased abundance of Lm facies. It is thick-bedded (>1 m) and gastropod-bearing, and it alternates with gray-to-white mudstone and marl (Fmm). Locally euhedral centimeter-sized gypsum crystals in beige marl occur (Facies G). The youngest subassociation (LFA2) is typical in the Karacaören log and is composed of Smf and thinner Fmm facies. The Smf is fossiliferous, locally bioturbated (*Ophiomorpha* isp. and *Skolithos* isp.) and displays symmetric ripples.

4.2. Late Pliocene-Quaternary infill (Karacasu formation)

Except for the recent deposits formed by axial drainages, the Late Pliocene to Quaternary deposits (Karacasu Formation) are widespread only in the Karacasu graben. Since the outcrops of the unit to the north of Yenice and

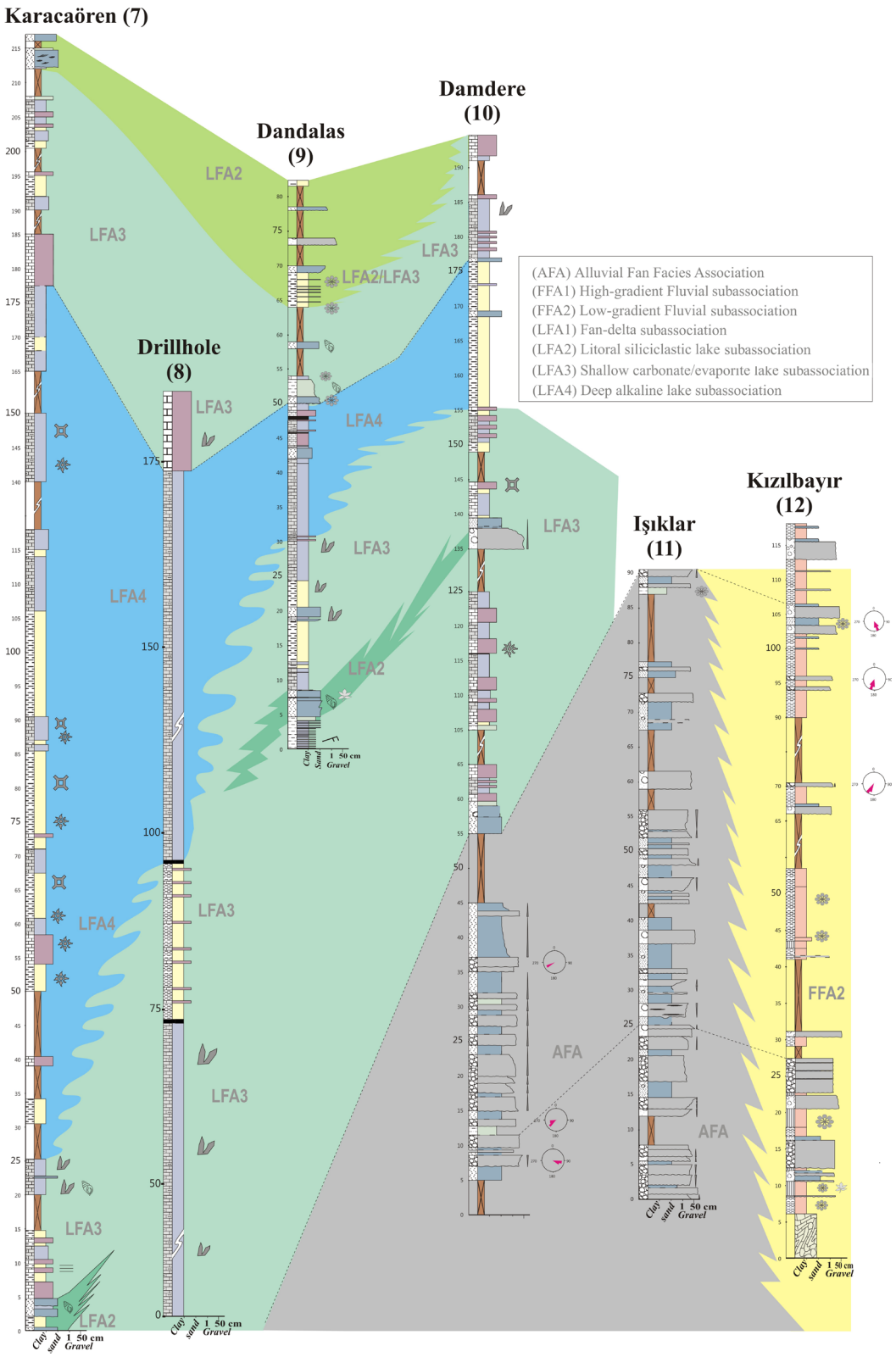


Figure 8. Measured sections from the Karacasu graben (see Figure 5 for locations of logs).

Olukbaşı villages in the Bozdoğan graben are limited, they are not considered here.

Sedimentological features of the Karacasu formation were studied in 3 sedimentological logs, namely the Dandalas-2 and Petrol logs to the west and Karındere log to the east of the Dandalas creek (Figures 5 and 9). The Dandalas-2 and Karındere logs have comparable facies attributes, which are characterized by considerable amount of fine-grained facies (Fl and P), alternating with massive to cross-bedded sandstones (Sm, Sp, St) and conglomerates (Gc) (Figure 9). The color of the facies Fl ranges from yellow to pink. Fine lamination of mudstone and siltstone is rarely preserved due to intense development of irregular calcrete nodules. *Equus stenonis and Bos* sp. fragments are found within this facies in the Dandalas-2 section (Figure 9). Facies Sp and St are thin (<1 m), laterally discontinuous (<10 m), and locally heavily influenced by calcrete development, too. Clast-supported conglomerate (Gc) is thicker (>2 m), laterally continuous (tens of meters), and massive to crude-bedded. Imbrication of gravels is a common feature. The size of gravel is mostly <5 cm, but it becomes larger (up to 35 cm) in the Karındere and Petrol logs. It is overlain by massive gray to yellow sandstone facies (Sm) forming together fining-upward cycles 4–6 m thick. Gravel imbrications from different levels indicate paleoflow directions towards the east and north in the Dandalas-2 and Petrol sections and the west in the Karındere section (Figure 9). An intense downward decreasing reddening at the top of each section is also seen in the Karacasu formation.

Facies features of the Karacasu formation can be attributed to the high-gradient fluvial subassociation (FFA1) related to lateral alluvial fans. The paleocurrent pattern verifies this interpretation. A considerable amount of fine facies near the center of the graben (Dandalas-2 log) would indicate an ancient axial low-gradient fluvial subassociation.

4.3. Synthesis of basinfill evolution

The suggested basinfill architecture of the Karacasu and Bozdoğan grabens, based on the distribution of facies associations, mostly relies on a simplistic graben model that is characterized by alluvial fans at the basin margin and lacustrine to fluvial sediments at the central trough.

In the lowermost reachable levels (Tortonian) of basinfill, basic outlines of grossly N-S–running grabens should have been already developed regarding the distribution of facies associations and paleocurrent directions (Figures 6 and 8). Subdued N-S trending elevations and bordering terrestrial Miocene sediments on the Madran horst near Örentaht and Örtülü probably belong to this early basin configuration (Figure 10a). Some intrabasinal topographic irregularities are suggested between Olukbaşı and Güvenir based on abrupt facies and thickness changes, and especially the occurrence of laterally discontinuous fan-delta sediments (Figure 10a). Separated by some basement uplifts, the graben floor was covered by shallow carbonate-evaporite lakes and fluvial sediments. Slumped carbonate intervals in the Baraj-1 and Kavaklı sections close to N-S border faults verify their activity at the time of deposition. The Karacasu graben was wider at the beginning with widespread alluvial and fluvial facies associations in the east (Figure 10a). At the end of the Messinian, the lacustrine system in the Bozdoğan graben was entirely replaced by an axial fluvial system (Medial Fluvial Package in Figure 6) and correlative lateral alluvial fans. Limited paleocurrent data prove that it flows northward (Figure 10b). Loci of deposition migrated basinwards in the Karacasu basin due to activation of inner faults, but widespread fluvial cover did not develop all over the basin, probably as a result of limited drainage area in the east. In the Early Pliocene, the lacustrine system, which is always characterized by shallow carbonate/evaporate facies association, attains its maximum extent (Figure 10c). In this period, relatively deeper lacustrine facies in the center of the Karacasu graben were encircled by shallow carbonate/evaporate facies belt. According to Alçiçek and Jimenez-Moreno (2013), a steppe climate characterized by widespread occurrence of *Artemisia* and limited arboraceous cover in lake-margin wetlands dominated in the region. Stable isotope data provided by the same authors demonstrated climate variations that could be comparable to larger-scale deepening and shoaling trends in the Karacasu basin (Figure 8).

Following a basinwide (probably even regional; see Section 6) unconformity in the late Early Pliocene, the basin configuration was not altered significantly (Figure 10d). The central trough was covered by fluvial facies, and lateral alluvial fans were wider compared to the previous period in the Karacasu graben. The axial fluvial system was flowing northwards, probably due to higher tectonic subsidence in the Büyük Menderes trough. Alçiçek and Jimenez-Moreno (2013) suggested a drier climate based on stable isotope data from interbedded calcrete horizons. Scarce preserved outcrops of the Karacasu formation in the SE of the Bozdoğan graben indicate that a similar configuration would have been valid in this basin, as well.

5. Graben tectonics

5.1. Description of the main faults

The mappable structural elements of the Karacasu and Bozdoğan grabens are shown in Figure 11. The western boundary of the Bozdoğan graben is defined by 3 major faults, including the Bozdoğan fault in the north, the Kamışlar fault in the center, and the Güvenir fault in the south. These faults meet each other at high angles (Figure 5). The Bozdoğan fault extends for 18 km N-S with a

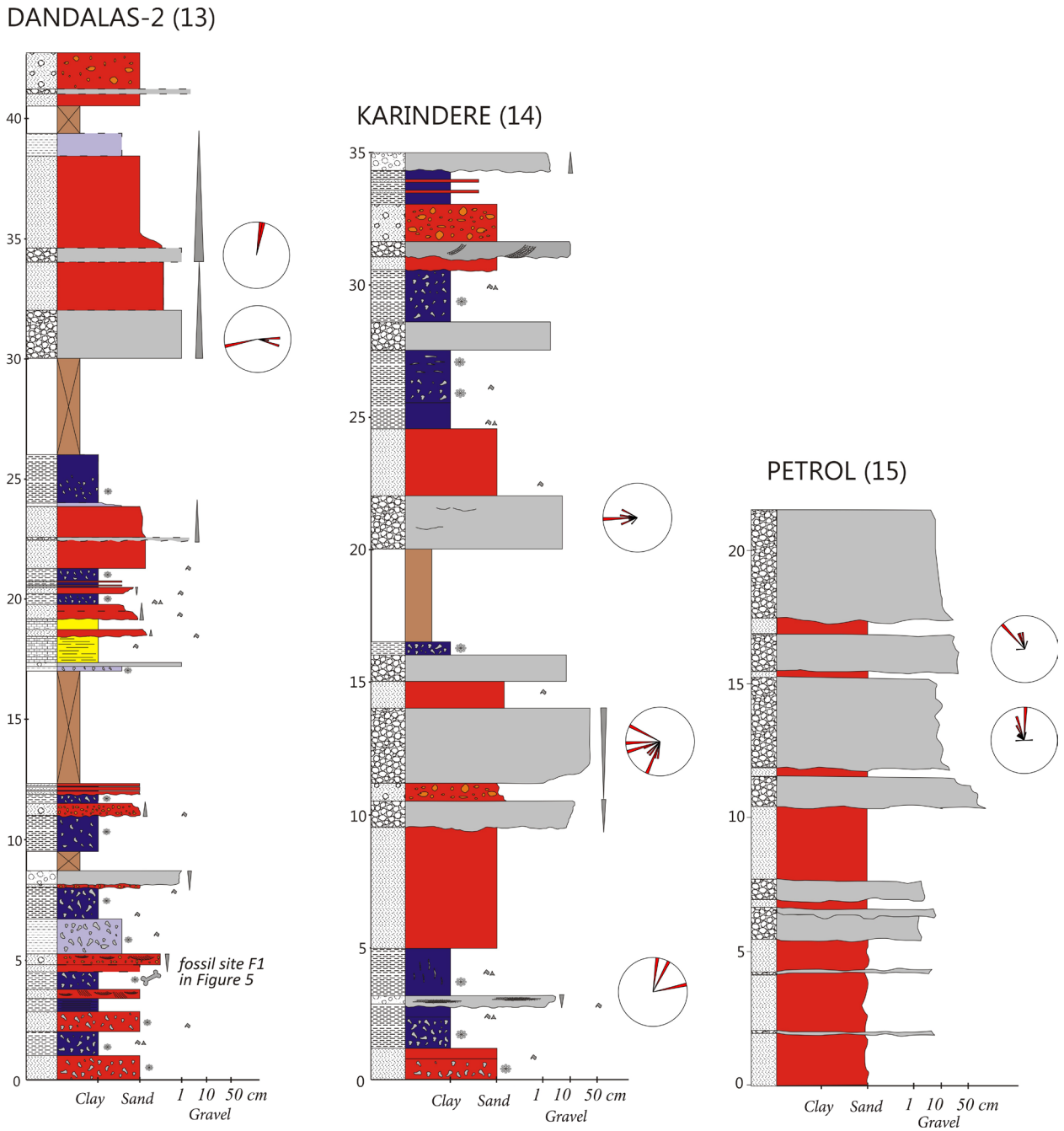


Figure 9. Sedimentological logs from the Quaternary alluvial fan complex from the Karacasu Graben (see Figure 5 for locations of logs).

curvilinear plan view from the northern tip of the graben to Bozdoğan in the south. This fault consists of several left and right stepping segments of 3–5 km long. Throughout the fault trace, Mio-Pliocene infill and reddish Quaternary gravel are tectonically juxtaposed with the metamorphic basement (Figures 12a and 12b). North of Osmaniye and near the northern tip, well-developed triangular facets indicate a vertical offset of at least 100 m. As previously stated, modern alluvial fans (some of which were already slightly incised) accompany the fault, particularly in the northern region (Figure 12c). At Bozdoğan, the graben margin suddenly deflects, extends for another 18 km N40-50W, and approaches the E-W trend at the SE tip. This segment is called the Kamışlar fault. Here, the mountain front sinuosity is significantly less, particularly in the SE portion relative to the Bozdoğan fault (Ocakoğlu et al.,

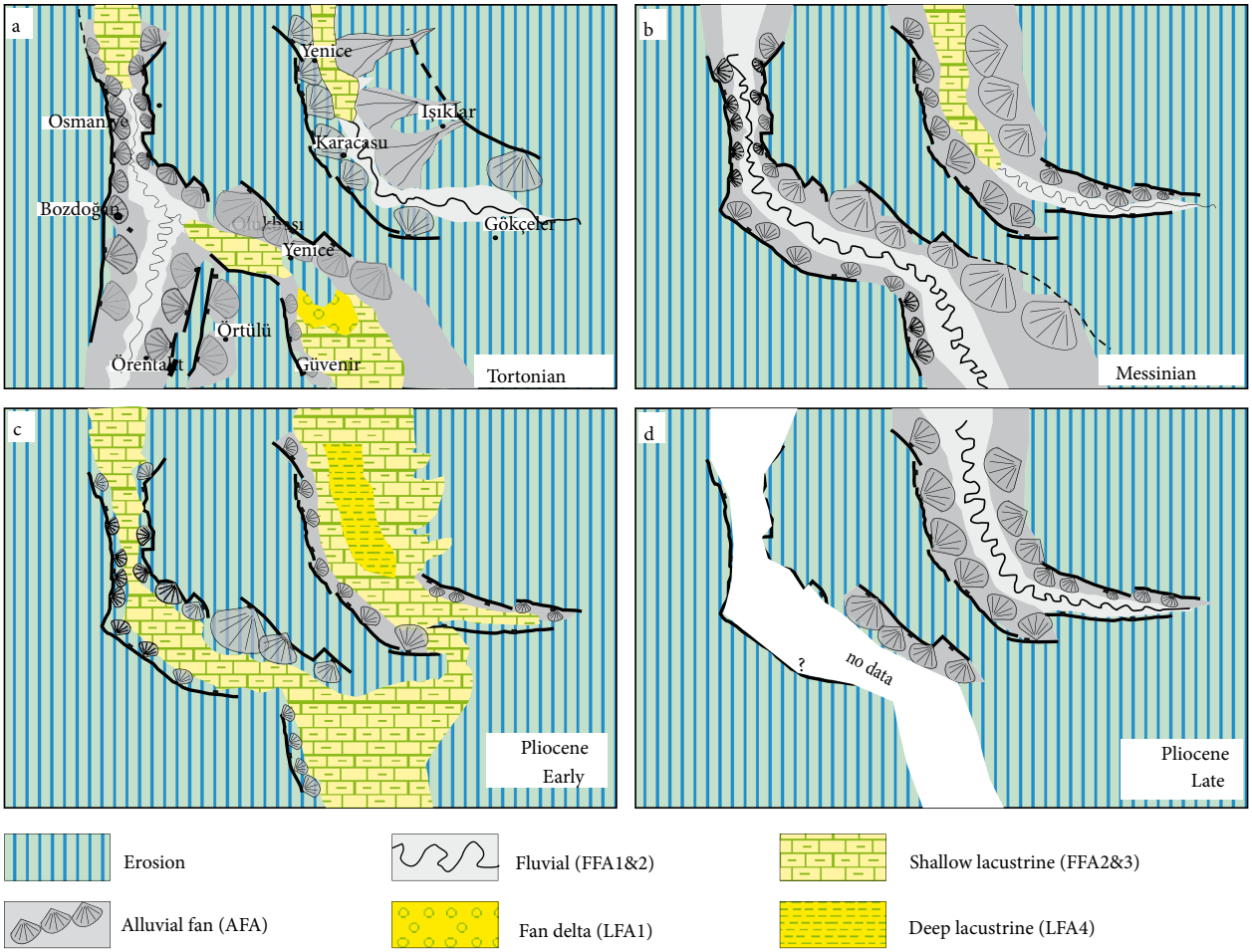


Figure 10. Paleogeographic maps of the Karacasu and Bozdoğan grabens. (a) Tortonian, (b) Messinian, (c) Early Pliocene, (d) Late Pliocene.

2007). Clear slickenside measurements near Bozdoğan indicate the presence of a normal slip with a slight dextral component (location 3 in Figure 11). In addition, 200 m south of Kamışlar, a reverse-to-thrust fault occurred between the metamorphic basement and the Mio-Pliocene lacustrine sediments (Ocakoğlu et al., 2007, p. 145). This segment has a complex structural history.

The Güvenir fault trends in the NW direction and across the western margin of the Kemer Hydroelectric Dam. This fault appears to have been exhumed by the deep and selective erosion of the Akçay creek (Figure 5). The Mio-Pliocene terrestrial and lacustrine sediments are tectonically confronted against the stiff basement metamorphic rocks throughout the fault trace. However, no morphological evidence is available that shows modern activity. Another fault set that is subparallel to the Güvenir fault and occurs in southwest Bozdoğan and Sırma is noteworthy (Figures 5 and 11). This fault is noticeable due to the straight mountain front in the middle of the metamorphic terrain. The westernmost fault of this set occurs NW of Örentaht and is nearly a continuation of the Bozdoğan fault. This type of fault is consistent with a highly steep scarp. In the east and between Örentaht and Örtülü, 2 lineations (adversely dipping normal faults) resulted in a horst structure (Figures 5 and 11). The eastern and western sides of this horst include a thin veneer of Mio-Pliocene fluvial sediments, which are the correlatives of the upper portion of the Bozdoğan graben basinfill (Figure 5; Ocakoğlu et al., 2007).

The eastern border of the Bozdoğan graben is defined by 2 distinctly different faults (Figure 5). The northern fault is situated more basinwards and is composed of a number of short (2–4 km) segments. Except for the linearity of the boundary between the infill and the basement and the apparent morphology, no direct evidence was gathered from this fault. However, the onlap of the patchy Mio-Pliocene deposits against the steep slopes of these lineaments provides indirect evidence (Figure 5.23 in Ocakoğlu et al., 2007). In the southeast, far from the basin axis and near Kızılcaköy, a second fault that is made up

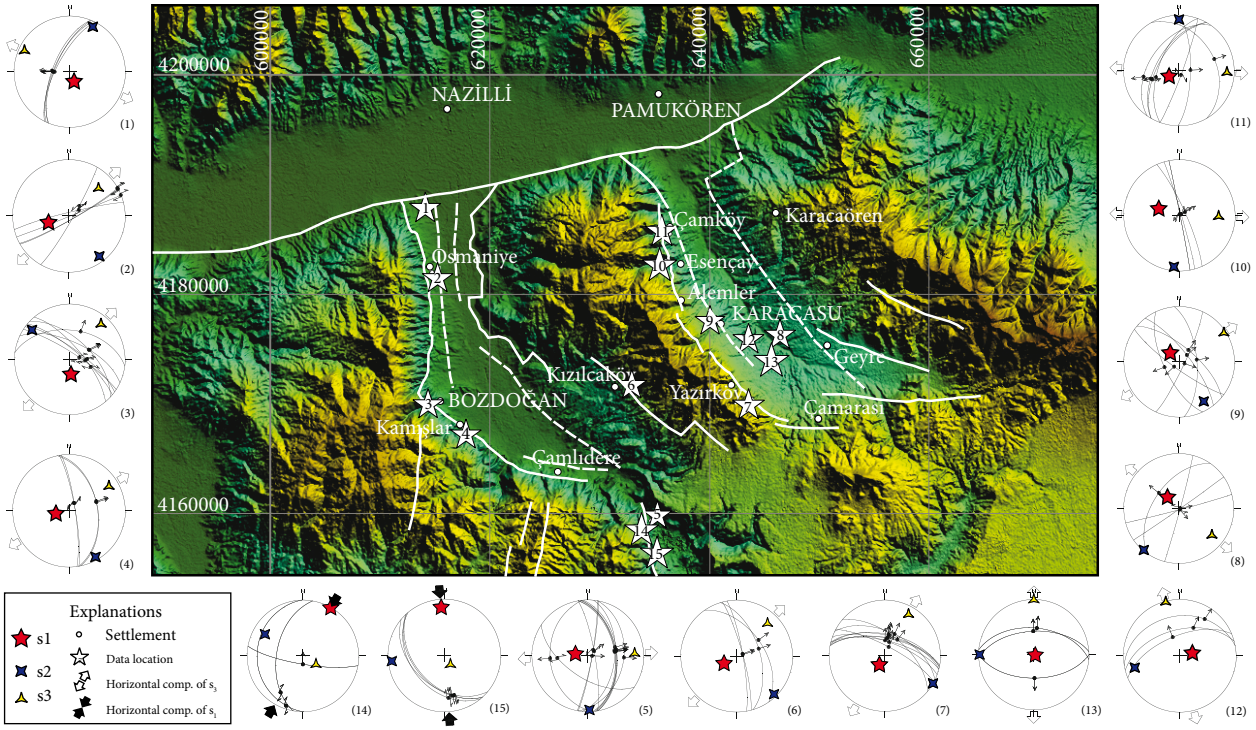


Figure 11. Shaded relief map (SRTM 30-m grid) showing the sites of stations where slip-data were measured and the stereographic plots of fault slip-plane data on the Schmidt lower hemisphere. σ_1, σ_2, and σ_3 represent the principal, intermediate, and least stress axes, respectively.

of 2 segments that are bound by high angle relay ramps occurs and follows a N50W trend (Figure 5). This fault is morphologically apparent and juxtaposes Mio-Pliocene and Quaternary alluvial fan deposits with a metamorphic basement. Several slickenside measurements indicated nearly pure dip-slip movement (Figure 11).

Structural features of the Karacasu graben are less obvious, likely due to lower denudation rates (except at the western margin fault, the Karacasu fault). The Karacasu fault begins with a segment that runs N30W and splays out from the southern border fault of the BMG north of Çamarası. This fault is associated with recent alluvial fans and elongated ridges in the metamorphic basement (Figure 5). In North Çamarası, the Karacasu fault turns N10W before it is gradually diverted northwestward and southward in 5 closely spaced stepping segments. Across the fault trace, the Mio-Pliocene and the Quaternary infill tectonically moved with the metamorphic basement (Figures 12d and 12e). Morphotectonic features of the modern activity, including triangular facets and the recently developed alluvial fans, gradually decreased southward and nearly disappeared in the E-W–running southeastern tip.

East of the Karacasu graben, the lineaments are diffuse. The N70W-trending Geyre fault delimits the graben floor from the basement rocks with an obvious morphology difference. However, the apex of the modern alluvial fans climbs far over the highly indented footwall block, which results in a clear low mountain front sinuosity (Figure 5; Ocakoğlu et al., 2007). As previously discussed for the basement morphology unit, a buried fault, which is likely an extension of the Geyre fault, continues northwestward beneath the Mio-Pliocene infill (Figures 3 and 5). Apart from them, additional NW-trending morphological lineaments that were developed on the stiff basement rocks east of Işıklar occur (Figure 5). We hypothesized that these lineaments are geometrically and stratigraphically similar to the long NW-running segments in the SE region of the Bozdoğan graben.

5.2. Paleostress analysis from slickensides

The paleostress analysis results that were derived from the slickenside measurements from the border faults and solitary faults in the basinfill are shown in Figure 11. A total of 79 slip data points were measured from the fault planes at 15 stations to calculate the principal stress directions and to determine the different deformational regimes.

Angelier's direct inversion method (version 5.42) was used to analyze the fault-slip data (Angelier, 1991). These results are presented on a Schmidt lower sphere stereographic projection. To define the paleostress field, the nature of the vertical/subvertical stress axis and the value of the φ ratio were considered (Angelier, 1994).

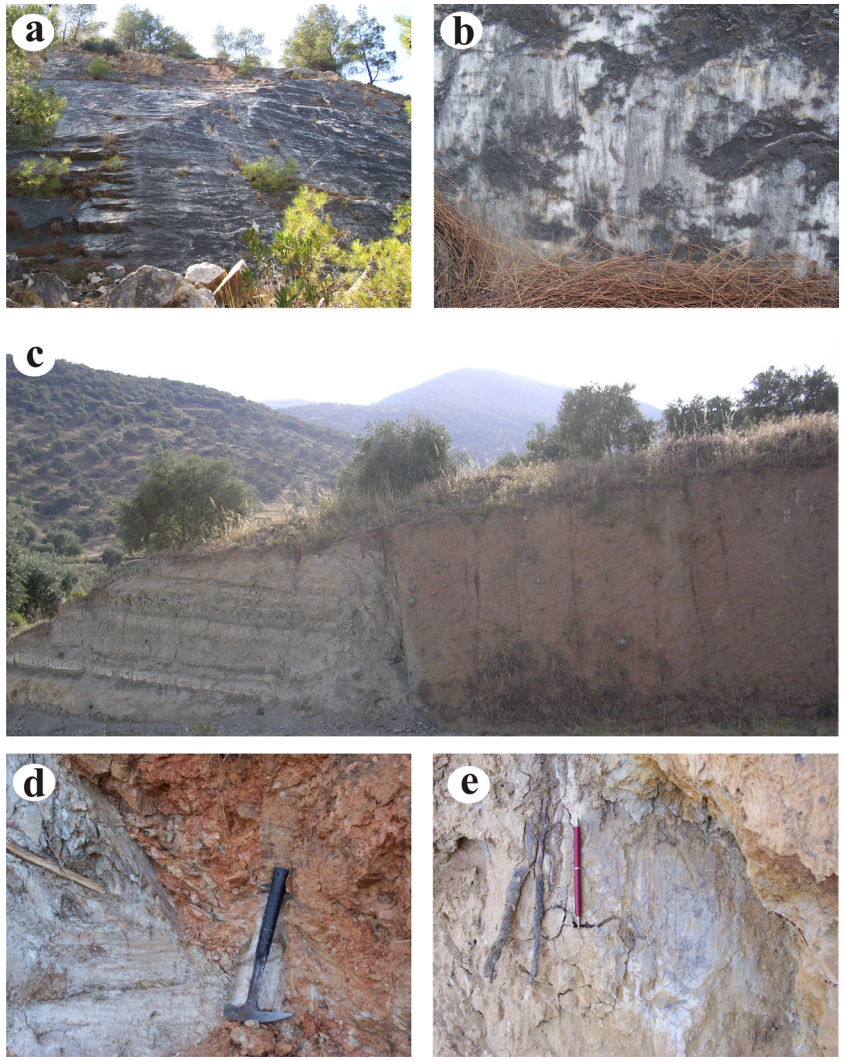


Figure 12. View of some fault planes from the Bozdoğan and Karacasu grabens. (a) Fault plane developed on marbles near the Akçay dam (location 5 in Figure 11) with almost pure normal slickensides (b). (c) Fault plane that separates lacustrine sediments from alluvial sediments (location 2 in Figure 11). (d) Karacasu fault between basement schists and Late Pliocene alluvial sediments (W of Karacasu town). Slickensides on this fault plane indicate almost pure dip-slip (e).

Stress fields may vary from radial extension (σ1 vertical, $0 < \varphi < 0.25$), extension (σ1 vertical) with pure extension ($0.25 < \varphi < 0.75$), and transtension ($0.75 < \varphi < 1$) to strike-slip stress fields (σ2 vertical) with pure strike-slip ($0.25 < \varphi < 0.75$), transtension ($0.75 < \varphi < 1$), and transpression ($0 < \varphi < 0.25$), or to compression (σ3 vertical) with pure compression ($0.25 < \varphi < 0.75$) and transpression ($0 < \varphi < 0.25$) (Delvaux et al., 1997). Radial compression (σ3 vertical, $0.75 < \varphi < 1$) was rejected from the calculation because it was considered as inconclusive.

Based on these results, we distinguished 5 different stress fields in the studied grabens. The first data set corresponds to the E-W–oriented tensional stress regime. Faults of this set are observed at the boundaries of the studied grabens where the basement units juxtapose the Miocene sediments and the older colluvial sediments. At stations 5, 10, and 11, s_1 is vertical and the f values represent the pure tensional stress regime (Figure 11).

The second data set indicates a NE-SW–directed tensional regime (stations 2, 3, 4, 6, 7, and 9) and is related with the Mio-Pliocene basinfill. In addition, s_1 is vertical for all stations. The f ratios of stations 2 and 4 indicate pure tensional stress regimes whereas stations 3, 6, 7, and 9 have radial extensive stress (Figure 11).

The third data set belongs to the N-S–oriented tensional regime and is observed in the Plio-Quaternary

basinfill units. This tensional regime was only observed at stations 12 and 13. Based on the f value, the stress regime is pure extensive where the s_1 is vertical (Figure 11).

The fourth data set is for the NW-SE tensional stress regime and was calculated from stations 1 and 8. The faults in this data set were observed at the margin of the Karacasu graben and in the basinfill. The s_1 was vertical for all stations and the f values of the 2 locations indicated a radial extensive stress regime (Figure 11).

The fifth data set represents the NE-SW compressional regime and was calculated at stations 14 and 15. The fault planes related to this regime were observed at the western boundary of the Bozdoğan graben in the far south (Güvenir fault), where the basement and the Miocene lacustrine units juxtapose. The s_1 is horizontal and the f value of this data set indicated pure compression (Figure 11).

5.3. Interpretation of the paleostress analyses

The field observations of the macro- and mesoscale faults and the paleostress analyses clearly document the different tension orientations for nearly every station in the study area (except stations 14 and 15). To determine the order of the phases, the stratigraphic units at the footwall and hanging wall of the fault planes were considered. The results of the paleostress analyses were divided into 4 main groups, including E-W–oriented tensional (stations 1, 5, 10, and 11), NE-SW–oriented tensional (stations 2, 3, 4, 6, 7, and 9), N-S–oriented tensional (stations 12 and 13), and N-S compressional stress field (14 and 15) groups. At station 8, the paleostress analyses indicated a NW-SE tensional stress regime that was not compatible with the 4 main groups. This station is thought to represent a local stress field change that was potentially generated during the N-S extension.

Previous studies clearly indicated a N-S to NNW-SSE modern tensional stress regime for the entire BMG (Angelier et al., 1981; Koçyiğit, 2005; Gürer et al., 2009). In addition, the focal mechanism solutions of the recent earthquakes located in the BMG support this ongoing extension (Ocakoğlu et al., 2013). Due to this evidence, most of the N-S–oriented tensional stress regime (the fault planes of stations 12 and 13 cutting the Plio-Quaternary units) is accepted as the last tectonic phase.

At stations 5, 10, and 11, the stress fields represent nearly pure E-W tension based on the f values, which indicated a single tension direction. In addition, these stations are located on the nearly N-S–trending faults of Bozdoğan, Karacasu, and Güvenir. Because these faults are perpendicular to the main BMG trend and show a single direction of tension, this phase is regarded as the first stage. Station 1 is an exception because it exhibits radial tension while showing the same tension direction (the change in the stress field character from pure to radial tension is thought to be related to the position of this location near the southern boundary fault of the BMG). Related fault planes of this phase were mainly observed between the basement units and the Miocene lacustrine sediments.

At stations 3, 6, 7, and 9, kinematic analyses indicated that the radial tension (according to f values) represented multidirectional extension with dominant NE-SW orientation. This phase is regarded as the second phase, which corresponds to the transitional stage of the E-W–oriented pure tensional stress regime to the N-S–directed one. In this group, stations 2 and 4 indicate a pure tensional stress regime that may result from insufficient fault plane data.

The fourth group of the paleostress analysis corresponded to a nearly N-S compressional stress regime. In addition to the Güvenir fault, a series of strike-slip faulting with reverse components and a pure reverse fault were observed and analyzed. This compressional phase is thought to have generated the E-W–oriented tensional stress regime as a local stress field between the basement units and the Miocene lacustrine sediments of the basinfill.

6. Discussion and conclusions

Our investigations in the K&B basins basically revealed the N-S–running grabens that initiated before the Late Miocene times under E-W extension and related N-S contraction. The grabens comprise 3 successions — a thick (~1100 m) Miocene-E. Pliocene fluviolacustrine unit, a thinner (~150 m) Late Pliocene-Quaternary alluvial-fluvial unit, and late Quaternary modern valley fill and terraces — that are separated from each other by regional unconformities. The structural data demonstrate that the dominant extension direction changed from E-W to N-S, as well.

The 3-fold nature of the infill of the neighboring BMG separated by unconformities was previously shown by many researchers (Paton, 1992; Cohen, et al., 1995; Bozkurt, 2000; Gürer et al., 2009; Çiftçi et al., 2011; Sümer et al., 2013; Koçyiğit, in press). The lowermost sequence consists of alluvial sediments and overlying lacustrine deposits (Gürer et al., 2009) and is dated to the Early-Middle Miocene based on mammalian, pollen, and magnetostratigraphic data (Ünay et al., 1995; Akgün and Akyol, 1999; Sarıca, 2000; Sarıca-Filoreau, 2002; Şen and Seyitoğlu, 2009). Koçyiğit (in press) stratigraphically positioned the lacustrine deposits to the north of Nazilli in the Late Miocene (Figure 1). Accordingly, these lacustrine levels are lithologically correlated with the lowermost observable lacustrine sediments of the Bozdoğan basin having mammalian fauna of Tortonian age (MN9) (Figures 4 and 5; F5 in Table 1). Regarding the existence of ~400-m-thick sediments below the present ground surface (see Section 2), it is reasonable to assume that older buried infill of the Bozdoğan graben would be

dated back to the Early Miocene. The structural context of the lower sequence in the BMG is disputable. Many researchers (Seyitoğlu and Scott, 1991, 1992; Cohen et al., 1995; Yılmaz et al., 2000; Göğüs, 2004; Çemen et al., 2006; Şen and Seyitoğlu, 2009; Çiftçi et al., 2011; Koçyiğit, in press) suggested a supradetachment basin setting related to the Büyük Menderes Detachment based on overall stratigraphy and sequence of regional events (Figure 1). Thermochronologic data support this view by showing the cooling of the Menderes Metamorphic Core Complex in the Early-Middle (!) Miocene (Gessner et al., 2001; Ring et al., 2003; Gessner et al., 2013). Contrarily, Gürer et al. (2009), using detailed geological mapping and structural analysis, revealed NE and NW running basins that were controlled by strike slip faults in an overall N-S contractional (and related E-W extensional) frame (Figure 13). The authors thought that this contraction continued until early Pliocene times and was caused by the emplacement of Lycian nappes related to late postcollisional intracontinental convergence. This explanation was also applied to the formation of the Muğla-Yatağan basin in the south (Figure 1; Görür et al., 1995; Gürer and Yılmaz, 2002). In the Söke basin further west, fluviolacustrine deposition in a supradetachment basin in the Early-Middle Miocene followed by late Miocene lacustrine sedimentation in a high angle normal fault-controlled basin were reported (Figure 1; Sümer et al., 2013). The Denizli basin in the east in the Middle Miocene-Early Pliocene experienced N-S (and partly NNW-SSE) extension (Koçyiğit, 2005) or alternatively bimodal NE and NW extension (Kaymakçı, 2005). Structural data collected from the K&B grabens indicate E-W extension (and related N-S compression), parallel to Gürer et al.'s (2009) findings (Figure 13).

A short-lived mid-Pliocene contraction in the BMG and nearby basins is observed (Figure 13). The suggested compression direction at this time varies from N-S to NE-SW. This would be the cause of angular unconformity between the lower and middle sequences in the K&B basins. Evidence for this contraction was collected from many other West Anatolian locations (Angelier et al., 1991; Koçyiğit et al., 1999; Bozkurt and Rojay, 2005; Rojay et al., 2005), and it is related to the contraction phase of Mercier (1981) in the Aegean Arc (Sümer et al., 2013).

The medial sequence over the mid-Pliocene unconformity in the BMG consists of Late Pliocene-Quaternary alluvial and fluvial deposits (the Kestel formation of Koçyiğit (in press) and Subunits B1 and B2 of Gürer et al. (2009)). It is correlated with the Karacasu formation in terms of lithology and age in the K&B basins (Figure 4). Structural and sedimentological data from the BMG indicates that this medial sequence was formed and back-tilted in a supradetachment basin related to the Büyük Menderes Detachment (Gürer et al, 2009; Koçyiğit, in press). Thermochronologic data demonstrated the highest movement rates on the Büyük Menderes Detachment from the Pliocene onward (Gessner et al., 2001; Ring et al., 2003) and support the field data above. Neighboring basins in this period underwent N-S and NNE-SSW extension, too

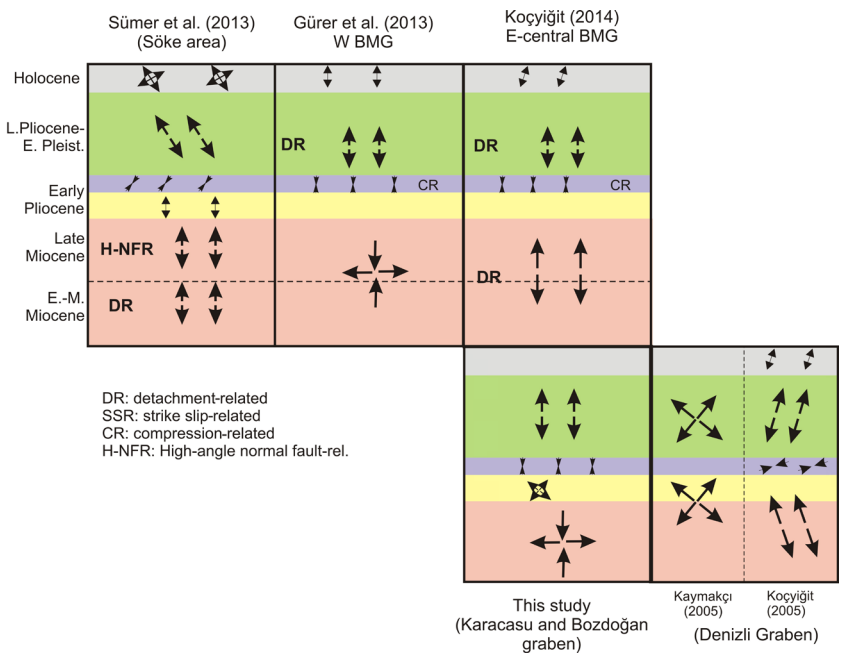


Figure 13. Panel showing the paleostress orientations in the vicinity of the BMG since the Early Miocene.

(Figure 13). Involvement of large-scale strike-slip structures in the Söke basin resulted in a local extension field in the NW-SE direction at this time (Sümer et al., 2013).

The upper sequence in the BMG (the Feslek formation of Koçyiğit (in press) and Unit C of Gürer et al (2009)) is still developing under the control of high angle normal faults under the modern N-S to NNE-SSW extension directions (Figure 13). Correlatives of this sequence in the K&B basins are erosion surface on KYK and valley fill and terrace deposits. It was previously suggested that the latter developed in close relation to modern subsidence in the BMG (Ocakoğlu et al., 2005). The cause of the modern extension is regarded as westward tectonic escape of the Anatolian platelet through border transform faults, as suggested by many authors (Bozkurt, 2000; Gürer et al., 2009).

Sedimentological and structural data from the K&B basins allow the following conclusions.

1. These grossly N-S–running long and narrow depressions are filled with more than 1100-m-thick Miocene to Quaternary sediments and are controlled by dominantly normal faults. Except for basinwards migration of control faults, no considerable geometric/morphological variation occurred in basin configuration.

2. Correlation of stratigraphic units and available mammalian age data with the BMG indicates that the lowermost stratigraphic intervals in the K&B basins at –300 m would be as old as the Early Miocene.

3. Facies peculiarities of the reachable middle and upper stratigraphic levels of the K&B basins obey a simple symmetric graben model in terms of infill architecture. This model comprises some intrabasinal structural irregularities and is characterized by alluvial/colluvial fans at basin margins, and fluvial and lacustrine facies associations at the center of the basins. The basin floor was covered by intertonguing lacustrine and fluvial facies associations in the Tortonian; by fluvial facies associations, especially in the Bozdoğan basin, in the Messinian; and mostly by shallow carbonate/evaporate lake facies associations in the Early Pliocene. Following a regional unconformity, widespread lateral alluvial fans and a north-heading (towards the BMG) axial fluvial system developed in the Late Pliocene-Early Quaternary.

4. Paleostress analysis of faults developed on different lithostratigraphic units revealed an E-W extension (and related N-S compression) in the Late Miocene, multidirectional extension that dominated in the NE-SW in the Early Pliocene, and N-S extension in the Late Pliocene-Quaternary. The first tectonic phase is connected with emplacement of the Lycian nappes in relation to late intracontinental convergence, while the latter phase is related to widespread extension on the Büyük Menderes Detachment as a consequence of westward tectonic escape of the Anatolian platelet. The second tectonic phase is considered a transitional phase in-between.

Acknowledgments

This paper is based on the findings of scientific projects numbered 200415022 and 201315c102, which were supported by the Commission for Scientific Research Projects of Eskişehir Osmangazi University, Eskişehir, Turkey. In addition, the authors are grateful for the logistic support of the Bozdoğan Municipality of Aydın Province during the 2006 summer season. The authors are particularly indebted to 2 anonymous referees who greatly improved the manuscript with their constructive suggestions.

References

Açıkalın S (2005). Sedimentary evolution of the Karacasu cross-graben (Aydın, West Anatolia). MSc, Eskişehir Osmangazi University, Eskişehir, Turkey (in Turkish with English abstract).

Akgün F, Akyol E (1999). Palynostratigraphy of the coal-bearing Neogene graben deposits in the Büyük Menderes, Western Anatolia. Geobios 32: 367–383.

Alçiçek H (2010). Stratigraphic correlation of the Neogene basins in southwestern Anatolia: regional palaeogeographical, palaeoclimatic and tectonic implications. Palaeogeography Palaeocl 291: 297–318.

Alçiçek H, Jiménez-Moreno G (2013). Late Miocene to Plio-Pleistocene fluvio-lacustrine system in the Karacasu Basin (SW Anatolia, Turkey): depositional, paleogeographic and paleoclimatic implications. Sediment Geol 291: 62–83.

Alçiçek H, Mayda S (2009). Sedimentological, mineralogical and geochemical investigation of the Karacasu Neogene Basin: an approach for the palaeogeographic and palaeoclimatic reconstruction (SW Anatolia, Turkey). Scientific Report No. ÇAYDAG 108Y097. Ankara, Turkey: Scientific and Technical Research Council of Turkey (in Turkish with English abstract).

Angelier J (1991). Inversion of field data in fault tectonics to obtain regional stress. III: A new rapid direct inversion method by analytical means. Geophys J Int 103: 63–76.

Angelier J (1994). Fault slip analysis and paleostress reconstruction. In: Hancock PL, editor. Continental Deformation. Oxford, UK: Pergamon, pp. 101–120.

Angelier J, Dumont JF, Karamanderesi H, Poisson A, Şimşek Ş, Uysal SŞ (1981). Analysis of Fault Mechanism and expansion of southwest Anatolia since the Late Miocene. Tectonophysics 75: T1–T9.

Barnes RA, Barnes WC (1978). Organic compounds in lake sediments. In: Lerman A, editor. Lakes: Chemistry, Geology, Physics. Berlin, Germany: Springer, pp. 127–152.

Becker-Platen JD (1971). Stratigraphic division of the Neogene and Oldest Pleistocene in Southwest Anatolia. Newsl Stratigr 1–3: 19–22.

Benda L, Meulenkamp JE (1990). Biostratigraphic correlations in the Eastern Mediterranean Neogene. 5. Calibration of sporomorph associations, marine microfossils and mammal zones, marine and continental stages and radiometric scale. In: 7th International Congress on Mediterranean Neogene, Athens, pp. 61–70.

Bentham PA, Talling PJ, Burbank DW (1993). Braid stream and flood-plain deposition in a rapidly aggrading basin: the Escanilla formation, Spanish Pyrenees. In: Best JL, Bristow CS, editors. Braided Rivers. London, UK: Geological Society of London Special Publication 75, pp. 177–194.

Blikra LH, Nemec W (1993). Postglacial avalanche activity in Western Norway: depositional facies sequences, chronostratigraphy and palaeoclimatic implications. In: Frenzel B, editor. Solifluction and Climatic Variation in the Holocene. Stuttgart, Germany: Gustav Fischer Verlag, pp.143–162.

Bluck BJ (1986). Upward coarsening sedimentation units and facies lineages, old Red Sandstone, Scotland. T RSE Earth 77: 251–264.

Bozkurt E (2000). Timing of extension on the Büyük Menderes Graben, western Turkey, and its tectonic implications. In: Bozkurt E, Winchester JA, Piper JDA, editors. Tectonics and Magmatism in Turkey and the Surrounding Area. London, UK: Geological Society of London Special Publication 173, pp. 385–403.

Bozkurt E, Oberhansli R (2001). Menderes Massif (Western Turkey): structural, metamorphic and magmatic evolution - a synthesis. Int J Earth Sciences 89: 679–708.

Bozkurt E, Rojay B (2005). Episodic, two-stage Neogene extension and short-term intervening compression in Western Turkey: field evidence from the Kiraz Basin and Bozdağ Horst. Geodin Acta 18: 299–316.

Candan O, Dora OÖ, Çetinkaplan M, Oberhansli R, Partzsch JH, Warkus FC, Durr S (2000). Pan-African high pressure metamorphism in the Precambrian basement of the Menderes Massif, western Anatolia, Turkey. Int J Earth Sciences 89: 793–811.

Çemen İ, Catlos EJ, Göğüs O, Özerdem C (2006). Postcollisional extensional tectonics and exhumation of the Menderes massif in the Western Anatolia extended terrain, Turkey. Geol Soc Am Bull Spec Pub 409: 353–379.

Çiftçi G, Pamukçu O, Çoruh C, Çopur S, Sözbilir H (2011). Shallow and deep structure of a supradetachment basin based on geological, conventional deep seismic reflection sections and gravity data in the Büyük Menderes Graben, Western Turkey. Sur Geophys 32: 271–290.

Cohen AS (2003). Paleolimnology: History and Evolution of Lake Systems. Oxford, UK: Oxford University Press.

Cohen HA, Dart CJ, Akyüz HS, Barka A (1995). Syn-rift sedimentation and structural development of the Gediz and Büyük Menderes graben, western Turkey. J Geol Soc London 152: 629–638.

Dağ F (1990). Aydın-Karacasu-Dandalas ÖİR: 2085 No'lu kükürt sahasının maden jeolojisi raporu, MTA Raporu, Derleme No: 8959. Ankara, Turkey: MTA (in Turkish).

Dean EW, Fouch TD (1983). Lacustrine environment. In: Scholle PA, Bebout DG, Moore CH, editors. Carbonate Depositional Environments. Tulsa, OK, USA: The American Association of Petroleum Geologists, pp. 97–116.

Delvaux D, Moeys R, Stapel G, Levi K, Miroshnichenko A, Ruzhich V, San'kov V (1997). Paleostress reconstructions and geodynamics of Baykal region. Tectonophysics 282: 1–4.

Emre T, Sözbilir H (1987). Field evidence for metamorphic core complex, detachment faulting and accommodation faults in the Alaşehir and Büyük Menderes grabens (western Turkey). In: Proceedings, International Earth Science Colloquium: Aegean Region, İzmir 1: 73–97.

Engesser B (1980). Insectivora und Chiroptera (Mammalia) aus dem Neogen der Turkei. Basel, Switzerland: Birkhäuser (in German).

Gaziry AW (1976). Jungtertiare Mastodonten aus Anatolien (Turkei). Geo. Jb. B.22:3-143, 2 abb. 2 tab. 16 taf. Hanover, Germany: E. Schweizerbart (in German).

Gessner K, Gallardo LA, Markwitz V, Ring U, Thomson SN (2013). What caused the denudation of the Menderes Massif: review of crustal evolution, lithosphere structure, and dynamic topography in southwest Turkey. Gondwana Res 24: 243–274.

Gessner K, Piazolo S, Güngör T, Ring U, Kröner A, Passchier CW (2001). Tectonic significance of deformation patterns in granitoid rocks of the Menderes nappes, Anatolian belt, southwest Turkey. Int J Earth Sciences 89: 766–780.

Göğüs O (2004). Geometry and tectonic significance of the Büyükmenderes detachment in the Bascayır area, Büyük Menderes graben, western Turkey, MSc, Oklahoma State University, Stillwater, OK, USA.

Görür N, Şengör AMC, Sakınç M, Tüysüz O, Akkök R, Yiğitbaş E, Oktay FY, Barka A, Sarıca N, Ecevitoğlu B et al. (1995). Rift formation in the Gökova region, southwest Anatolia: implications for the opening of Aegean Sea. Geol Mag 132: 637–650.

Gürer F, Yılmaz Y (2002). Geology of the Ören and surrounding areas, SW Anatolia. Turk J Earth Sci 11: 1–13.

Gürer ÖF, Sarıca-Filoreau N, Özburan M, Sangu E, Doğan B (2009). Progressive development of the Büyük Menderes Graben based on new data, western Turkey. Geol Mag 146: 652–673.

Harms JC, Southard JB, Walker RG (1982). Structures and sequences in clastic sequences in clastic rocks. Tulsa, OK, USA: Society of Economic Paleontologists and Mineralogists Short Course No. 9.

Hwang IG, Chough SK (1990). The Miocene Chunbuk Formation, southeastern Korea: marine Gilbert-type fan-delta system. In: Colella A, Prior D, editors. Coarse-Grained Deltas: Special Publication 10 of the IAS. Ghent, Belgium: IAS, pp. 235–254.

Hwang IG, Chough SK, Hong SW, Choe MY (1995). Controls and evolution of the fan delta systems in the Miocene Pohang Basin, SW Korea. Sediment Geol 98: 147–179.

Kastelli M (1972). Denizli-Sarayköy-Çubukdağ-Karacasu alanı jeoloji incelemesi, MTA Genel Müdürlüğü, Derleme No: 2532. Ankara, Turkey: MTA (in Turkish).

Kaymakçı N (2006). Kinematic development and paleostress analysis of the Denizli Basin (Western Turkish): implications of spatial variation of relative paleostress magnitudes and orientations. J Asian Earth Sci 27: 207–222.

Kim SB, Chough SK, Chun SS (1995). Blocky deposits in the lowermost part of the Cretaceous Kyokpori formation, SW Korea: cohesionless debris flows and debris falls in steep-gradient delta slope. Sediment Geol 98: 97–119.

Koçyiğit A (2005). The Denizli graben–horst system and the eastern limit of the western Anatolian continental extension: basin fill, structure, deformational mode, throw amount and episodic evolutionary history, SW Turkey. Geodin Acta 18: 167–208.

Koçyiğit A (in press). Role of Neotectonics in geothermal exploration: a case study in the Nazilli-Buharkent section of Büyükmenderes graben, SW Turkey. Geodinamica Acta.

Koçyiğit A, Yusufoğlu H, Bozkurt E (1999). Evidence from Gediz graben for episodic two stage extension in western Turkey. J Geol Soc London 156: 605–616.

Konak N, Göktaş F (2004). 1/100.000 ölçekli Türkiye jeoloji haritaları serisi, Denizli M21 paftası. Ankara, Turkey: MTA (in Turkish).

Kraus MJ (1999). Paleosols in clastic sedimentary rocks: their geological applications. Earth-Sci Rev 47: 41–70.

Lechman TM (1989). Upper Cretaceous (Maastrichtian) paleosols in Trans-Pecos Texas. Geol Soc Am Bull 101: 188–203.

Lips ALW, Cassard D, Sözbilir H, Yılmaz H (2001). Multistage exhumation of the Menderes Massif, western Anatolia (Turkey). Int J Earth Sciences 89: 781–792.

Mercier JL (1981). Extensional-compressional tectonics associated with the Aegean arc: comparison with the Andean Cordillera of south Peru-north Bolivia. Philos T R Soc A 300: 337–355.

Miall AD (1977). A review of the braided stream environments. Earth-Sci Rev 13: 1–62.

Miall AD (1978). Lithofacies types and vertical profile models in braided river deposits: a summary. In: Miall AD, editor. Fluvial Sedimentology, Canadian Society of Petroleum Geologists, Memoir 5: 597–604.

Nebert K (1955). Bozdoğan ve Karacasu'daki genç Neojen körfezleri, MTA Genel Müdürlüğü, Report no: 2511. Ankara, Turkey: MTA (in Turkish).

Nemec W, Postma G (1993). Quaternary alluvial fans in southwestern Crete: sedimentation processes and geomorphic evolution. In: Marzo M, Puigdefabregas G, editors. International Association of Sedimentologists Special Publication 17. Ghent, Belgium: IAS, pp. 235–276.

Nemec W, Steel RJ (1984). Alluvial and coastal conglomerates: their significant features and some comments on gravelly mass-flow deposits. In: Koster EH, Steel RJ, editors. Sedimentology of Gravels and Conglomerates. Canadian Society of Petroleum Geologists Memoir 10: 1–31.

Ocakoğlu F, Açıkalın S, Akan S, Saraç G, Dirik K (2005). Karacasu Çapraz Grabeni (Menderes Masifi) Dolgusunun Morfosedimanter Özellikleri, Yaşı ve Bölgesel Tektonik Açıdan Çağrışımları. In: Türkiye Kuvaterner Sempozyumu, 2–5 June 2005, İstanbul, Bildiri Özleri Kitabı (in Turkish).

Ocakoğlu F, Açıkalın S, Dirik K, Demirtaş R, Özsayın E (2007). Karacasu ve Bozdoğan Çapraz Grabenlerinin (Batı Anadolu) Stratigrafik, Sedimantolojik ve Tektonik Evrimi. Eskişehir, Turkey: Eskişehir Osmangazi Üniversitesi Araştırma Fonu, Proje no: 200415022 (in Turkish).

Ocakoğlu F, Açıkalın S, Güneş G, Özkes S, Dirik K, Özsayın E (2013). Was the 1899 Menderes Valley earthquake a double earthquake? Historical and paleosismological constraints. J Asian Earth Sci 67–68: 187–198.

Paton S (1992). Active normal faulting, drainage patterns and sedimentation in SW Turkey. J Geol Soc London 149: 1031–1044.

Platt NH, Wright WP (1991). Lacustrine carbonates: facies models, facies distribution and hydrocarbon aspects. In: Anadon P, Cabrera L, Kelts K, editors. Lacustrine Facies Analysis. Ghent, Belgium: IAS Special Publication 13, pp. 57–74.

Ratte C (2001). The urban development of the Aphrodisias in the Late antiquity. In: Parrish D, editor. Urbanism in Western Asia Minor. New Studies on Aphrodisias, Ephesos, Hieropolis, Pergamon, Perge and Xanthos. Portsmouth, RI, USA: Journal of Roman Archaeology, pp 139–147.

Retallack GJ (2001). Soils of the Past: An Introduction to Paleopedology. 2nd ed. London, UK: Blackwell Science Ltd.

Ring U, Johnson C, Hetzel R, Gessner K (2003). Tectonic denudation of a Late Cretaceous–Tertiary collisional belt: regionally symmetric cooling patterns and their relation to extensional faults in the Anatolide belt of western Turkey. Geol Mag 140: 421–441.

Rojay B, Toprak V, Demirci C, Süzen L (2005). Plio-Quaternary evolution of the Küçük Menderes Graben Southwestern Anatolia, Turkey. Geodin Acta 18: 317–331.

Rust RR (1978). Depositional model for braided alluvium. In: Miall AD, editor. Fluvial Sedimentology. Canadian Society of Petroleum Geologists Memoir 5: 133–145.

Rust RR (1984). Proximal braidplain deposits in the Middle Devonian Malbaie Formation of Eastern Gaspe, Quebec, Canada. Sedimentology 31: 675–695.

Saraç G (2003). Türkiye Omurgalı Fosil Yatakları. Rapor No. 10609. Ankara, Turkey: MTA (in Turkish).

Sarıca N (2000). Plio-Pleistocene age of Büyük Menderes and Gediz grabens and their tectonic significance on N–S extensional tectonics in West Anatolia: mammalian evidence from the continental deposits. Geol J 35: 1–24.

Sarıca-Filoreau N (2002). Faunes de rongeurs néogènes et quaternaires des grabens d'Anatolie occidentale. Systématique, biochronologie et implications tectoniques. PhD, Muséum National d'Histoire Naturelle, Paris, France (in French).

Schmidt-Kittler N (1976). Raubtiere aus dem Jungtertiar Kleinasiens. Palaeontographica Abt. A. 155, Lfg. 1-4, 1-131. Stuttgart, Germany: Schweizerbart (in German).

Schreiber BC, El Tabakh M (2000). Deposition and early alteration of evaporites. Sedimentology 47 (Suppl. 1): 215–238.

Şen Ş, Sarıca N (2011). Middle Late Miocene Spalacidae (Mammalia) from western Anatolia and the phylogeny of the Family. Yerbilimleri 32: 21–50.

Şen Ş, Seyitoğlu G (2009). Magnetostratigraphy of early–middle Miocene deposits from east–west trending Alaşehir and Büyük Menderes grabens in western Turkey, and its tectonic implications. In: Van Hinsbergen DJJ, Edwards MA, Govers R, editors. Collision and Collapse at the Africa–Arabia–Eurasia Subduction Zone. J Geol Soc London Special Publications 311: 321–342.

Seyitoğlu G, Scott BC (1991). Late Senozoic crustal extension and basin formation in West Turkey. Geol Mag 128: 155–166.

Seyitoğlu G, Scott BC (1992). The age of the Büyük Menderes Graben (West Turkey) and its tectonic implications. Geol Mag 129: 239–242.

Sickenberg F, Becker-Platen JD, Benda L, Berg D, Engesser B, Gaziry W, Heissig K, Hunermann KA, Sondaar PY, Schmidt-Kittler N et al. (1975). Die Gliederung des höheren Jungtertiärs und Altquartärs in der Türkei nach Vertebraten und ihre Bedeutung fur die Internationale Neogen-Stratigraphie. Stuttgart, Germany: Schweizerbart (in German).

Staesche U, Sondaar PY (1979). Hipparion aus Vallesium und Turolium (Jungtertiar) der Turkei. Geol. Jb. B. 33., 35-79. 26 Abb. 5 tab. Hanover, Germany: E. Schweizerbart (in German).

Sümer Ö, İnci U, Sözbilir, H (2013). Tectonic evolution of the Söke Basin: extension-dominated transtensional basin formation in western part of the Büyük Menderes Graben, Western Anatolia, Turkey. J Geodyn 65: 148–175.

Todd SP (1989). Stream-driven, high-density gravelly traction carpets: possible deposits in the Trabeg Conglomerate formation, SW Ireland and theoretical considerations of their origin. Sedimentology 36: 513–530.

Ünay E, Göktaş F, Hakyemez Y, Avşar M, Şan Ö (1995). Dating of the sediments exposed at the northern part of the Büyük Menderes Graben (Turkey) on the basis of Arvicolidae (Rodentia, Mammalia). Türkiye Jeoloji Bülteni 38: 75–80 (in Turkish with English abstract).

Valero-Garcés B, Morellon M, Moreno A, Corella JP, Martin-Puertas C, Barreiro F, Perez A, Giralt S, Mata-Campo MP (2014). Lacustrine carbonates of Iberian Karst Lakes: source, processes and depositional environments. Sediment Geol 299: 1–29.

Warren JK (2006). Evaporites: Sediments, Resources and Hydrocarbons. Berlin, Germany: Springer.

Yıldız MS, Özmen A, Sülün S (1986). Rejyonal Jeoelektrik Haritalama Projesi Nazilli-Kuyucak-Karacasu Sahaları Rezistivite Etüdü. MTA Genel Müdürlüğü Derleme No: 1980. Ankara, Turkey: MTA (in Turkish).

Yılmaz Y, Genç ŞC, Gürer F, Bozcu M, Yılmaz K, Karacık Z, Altunkaynak Ş, Elmas A (2000). When did the Western Anatolia Grabens begin to develop? In: Bozkurt E, Winchester JA, Piper JDA, editors. Tectonic and Magmatism in Turkey and the Surrounding Area. J Geol Soc London Special Publications 173: 353–384.